Scholars' Mine

Spring 1983

Mechanical properties of alumina for orthopedic implant use

Ho Tong Fang

Recommended Citation

MECHANICAL PROPERTIES OF ALUMINA

FOR ORTHOPEDIC IMPLANT USE

BY

HO TONG FANG, 1956-

A THESIS

Presented to the Faculty of the Graduate School of the

UNIVERSITY OF MISSOURI-ROLLA

In Partial Fulfillment of the Requirements for the Degree

MASTER OF SCIENCE IN CERAMIC ENGINEERING

1982

Approved by

Delbert E. Day (Advisor) _Robert E. Moore_

Roger F. Brown

PUBLICATION THESIS OPTION

This thesis has been prepared in the style utilized by the Journal of the American Ceramic Society.

ACKNOWLEDGEMENT

TABLE OF CONTENTS

TABLE OF CONTENTS (Cont.)

LIST OF ILLUSTRATIONS

LIST OF TABLES

ABSTRACT

The static fatigue, flexural strength and chemical corrosion of three commercially prepared, polycrystalline aluminas, two of orthopedic implant grade, were measured in demineralized water at 37°C and 70°C. The dissolution of a Ca-rich impurity phase, probably a glass, segregated at the grain boundaries and external surface, appears at least partially responsible for the significant difference in static fatigue of these three aluminas. The present results indicate that the minimum static fatigue in demineralized water, and the highest flexural strength in demineralized water and HF solution are both achieved by the alumina characterized by a low concentration of Ca at the grain boundaries and minimum Ca dissolution.

I. INTRODUCTION

The first clinical applications of aluminum oxide or alumina as a biomaterial were in the 1970's.[1] Current biomedical applications[2] include joint replacements, vertebrae spacers and extensors, and dental implants.

Alumina is used because of its favorable properties such as high strength, good wear and glide behavior,[1] biological inertness and compatability, and relatively low cost. Unlike metals, alumina does not suffer from galvanic corrosion in the physiologic environment of the human body, which is essentially an aqueous solution of approximately 0.15M NaCl containing organic acids, proteins, enzymes, biological macromolecules, electrolytes, and dissolved oxygen, nitrogen, and carbon dioxide.[3]

Similar to other ceramics, alumina exhibits static fatigue[4-7] or delayed failure, especially in the presence of water or moisture. The importance of moisture is illustrated by the results of tests with a 96% Al_2O_3 ceramic.[4] The data indicated that the mean lifetime decreased from 1400 min when tested in dry Ar (<2 ppm H_2O or O_2) to only 0.3 min in air of 50% relative humidity.[4] The fatigue lifetime also depends upon the testing temperature[4,5] and the magnitude of the applied stress.[5-7]

The fatigue, whether static or cyclic, of most materials is attributed[6] to the growth of subcritical microcracks which eventually leads to catastrophic failure. The time to failure for static fatigue, therefore, is often considered to be the time required for a crack to reach a critical size which satisfies the criterion for stable crack propagation. Fracture mechanics theory[8-10] offers a framework within which long-term lifetimes can be predicted from results of relatively short term tests. Various subcritical velocity equations, applicable to polycrystalline alumina have been developed which adequately represent the static fatigue data for the conditions investigated[12]. However, the exact mechanism or nature of the corrosion process, commonly believed to be responsible for subcritical crack growth in single crystal (sapphire) or polycrystalline alumina, is still not fully known. One possibility is the formation or lengthening of microcracks due to the reaction of Al_2O_3 with H_2O to form its hydroxide or its oxyhydroxide according to the reactions[13]:

$$Al_2O_3 + 3H_2O = 2Al(OH)_3$$
$$\Delta G° = -16.14 \text{ KJ/mole at } 25°C$$
$$\Delta G° = +8.10 \text{ KJ/mole at } 127°C \tag{1}$$

$$Al_2O_3 + H_2O = 2AlO(OH)$$
$$\Delta G° = -17.44 \text{ KJ/mole at } 25°C$$
$$\Delta G° = -11.40 \text{ KJ/mole at } 127°C \tag{2}$$
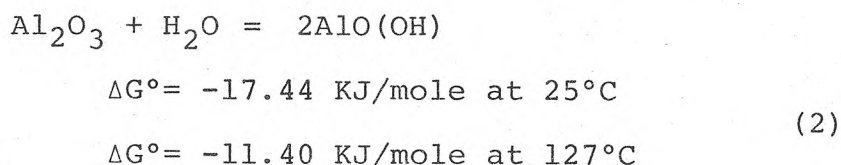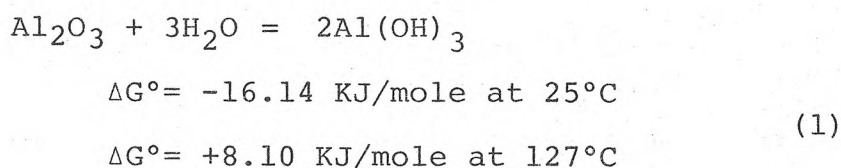
At 25°C, the thermodynamic free energy of formation indicates that both reactions are spontaneous, but at 127°C only reaction (2) is favored. The corrosion process could also involve reaction products of larger volume which create localized tensile stresses at the crack tip forcing the crack apart.

For polycrystalline aluminas containing a glass phase(s), crack growth might involve the dissolution of the glass,[11,14] which could weaken the intergranular bonding or increase the stresses at the crack tip by microcrack extension or crack tip sharpening. More than one process could be involved, some of which do not require water. Wiederhorn et al[15] used a previously proposed thermally activated crack growth process to qualitatively explain crack propagation in glass tested in vacuum.

Recent investigation[16-20] involving exposure of poly-crystalline alumina to saturated steam have added some new information concerning the corrosion process. The flexural strength of commercially produced dense aluminas was significantly lower[16-20] after exposure to saturated steam at relatively low temperatures (< 300°C) and, in some cases,[16-18] a signficant increase in the concentration of the Ca impurity in these aluminas was found at the free (external) surface. The Ca impurity present

in as-manufactured aluminas is known to be segregated initially at the internal grain boundaries[21-27] and concentrated on the surface of internal pores[25]. The Ca concentration can be 10-1000 times that of the bulk concentration[24-27], depending mainly on the thermal history (firing temperature and cooling rate) of the alumina in a manner consistent with equilibrium-segregation theory.[22,23] The segregation of Ca has been attributed to the size mismatch of the Ca^{2+} ion (0.99Å) and the Al^{3+} substitutional site (0.50Å)[24], which renders accommodation of Ca in the Al_2O_3 lattice energetically unfavorable resulting in segregation of Ca to free surfaces. In as-manufactured dense aluminas, Ca impurity segregation appears to lower the fracture toughness (K_{IC})[21,26], and to increase the tendency for intergranular fracture[21]. The segregation of other impurities at the grain boundaries of dense alumina has been observed less often. An increase in Si concentration was found at the external surface of aluminas after exposure to saturated steam[28,29] or reheating in air[30,31], but its migration appears to be slower than that for Ca[28].

In the present work, the migration of impurities, especially Ca, and the static fatigue of dense aluminas in demineralized water was investigated within the context

of the information showing that Ca migration was associated with a reduction in flexural strength for dense polycrystalline aluminas exposed to saturated steam. One objective was to determine the extent to which the Ca impurity was released from dense, high purity aluminas in contact with demineralized water at 37°C. There was also interest in determining whether the release of Ca could be related to the static fatigue characteristics of the aluminas. The strength reduction and impurity migration after aging the aluminas in water or dilute HF acid was also investigated.

Two of the aluminas investigated were high purity, (> 99.7% Al_2O_3) surgical implant grade. There has been only one aging experiment[32] and no static fatigue measurements on aluminas manufactured specifically for orthopedic use. Knowledge of the failure mechanism of these aluminas in an environment approximating the human body is essential to designing implant devices for long term use.

A less pure (99%) non-orthopedic grade alumina was also investigated based on the rationale that its reaction with water or aging solution might be more extensive and easily observed. Furthermore, the less pure alumina has been used in several previous studies.[16,19,28,29] Dilute HF acid was selected because of its well known ability to dissolve silicate glass, thereby accelerating any reaction with the intergranular glassy phase(s) present in the aluminas studied.

II. EXPERIMENTAL PROCEDURE

A. Sample Description

The impurity content and relevant properties of the three commercial aluminas investigated are listed in Table I. The two orthopedic implant grade aluminas, A and B, were both >99.7% Al_2O_3. Alumina C was of lower purity, 99% Al_2O_3, and was included for comparitive purposes. The only crystalline phase detected by X-ray diffraction (XRD) analysis of the three aluminas was α-alumina (corundum).

Alumina A specimens were injection molded cylindrical rods 3.311 ± 0.026*mm in diameter and 41.2 mm in length. Alumina B specimens were square bars 26.5 mm long, with a reduced cylindrical middle section 3.121 ± 0.021 mm in diameter, that had been cut and machined from dry-pressed plates. Alumina C specimens, 32.0 mm in length, were cut from extruded circular rods, 3.174 ± 0.004 mm in diameter, whose external surface appeared to have been ground after firing. The aluminas are estimated to have been sintered between 1500°C to 1600°C, but their exact thermal history is unknown.

---

* ± value corresponds to one standard deviation.

All alumina A and B specimens were washed successively in heptane, chloroform, ethanol, and ethyl ether, following the washing procedure described elsewhere.[32] Alumina C rods were washed successively in acetone and ethanol for 5 min in a ultrasonic cleaner. None of the specimens were washed with water, and all specimens were stored in vacuo.

B. Static Fatigue

The static fatigue apparatus used in the present study was similar to those described by Ritter et al.[33] The alumina rod knife edges of the three-point bending apparatus were identical to those used to measure the short term flexural strength. A constant static load was applied to the specimen with lead shot, via a single lever arm. Separate loading jigs were used for the simultaneous testing of 10 individual specimens. Each jig was calibrated by measuring the force exerted by the top knife edge when different weights were attached to the lever arm. The loading apparatus was mounted on shock absorbing materials to minimize vibrations and an isolated framework built around the apparatus arrested the falling lever arm at specimen failure. Failure times were recorded automatically, to the nearest 0.5 min, by a microswitch controlled electric

timer, which stopped at specimen failure. Failure times <2 min were measured with a stopwatch.

Fifteen to twenty specimens were usually used for each test in demineralized water (pH=5.6) at 37°C or 70°C (± 1°). Specimens immersed in demineralized water were loaded at 65% to 85% of their average failure load (AFL), based on their flexural strength when tested dry. Specimens that did not break in 14 days were collected and their flexural strength measured in air. Randomly selected, broken specimens from each test were examined by Auger Electron Spectroscopy (AES) and Scanning Electron Microscope (SEM). The water in which a specimen was immersed was analysed by Atomic Absorption Spectrophotometry (AAS).*** Impurities dissolved from the aluminas were undetectable, however, due to the large water to alumina specimen volume ratio ($\sim$100:1).

C. Aging Tests

Specimens were aged at 37°C and 70°C in demineralized water, dilute commercial grade HF acid solutions (1-8 wt% HF) and in air. The specimen and 2 ± 0.02 ml of liquid, measured with a precision pipette[†] with disposable polyethylene tip, were sealed in a thin ($\sim$0.05 mm), flexible

---

*** Model 560 Perkin-Elmer, Norwalk, Conn.
 † Finnepipette, Labsystem, Helsinki, Finland.

heat sealable plastic[††] container that did not affect the measured flexural strength of the alumina specimen. The specimen sealed in the plastic container was broken in three-point bending after the desired aging period, normally 7 days. Immediately after breaking a specimen, the liquid in the container was collected and stored in a polypropylene bottle. The broken specimen was removed quickly, washed in tap water and thoroughly rinsed in demineralized water to stop any further reaction, especially with the newly fractured surface. The liquids were analysed by AAS and randomly selected specimens from each group were later examined by AES, SEM, and X-ray diffraction (XRD).

Florescent dye[*] and food coloring[**] were used to detect liquid penetration into the alumina. The dyes were either added to the liquid, or aged specimens were immersed in the concentrated dye solution under pressure.

Specimens sealed in plastic containers containing demineralized water at 37°C were also aged under load (75% AFL for alumina A and 65% AFL for aluminas B and C) in the static fatigue apparatus. Any specimens that broke before the desired aging period were replaced or discarded.

[††] Dazey Product Co., Industrial Airport, Kansas.
[*] Fluorescene, MCP Reagent, Norwood, Ohio.
[**] Durkee, SCM Corporation, Cleveland, Ohio.

A companion specimen, also sealed in plastic, was aged alongside the stressed specimen, but without load. The alumina specimens used in the aging experiment requiring analysis of the liquid were chosen so that the weight differences between specimens in the same group were <1%.

D. Flexural Strength

The modulus of rupture (MOR) was measured in three-point bending at a strain rate of 0.5 mm/min in ambient air (∿35-55% rh) using alumina rods as knife edges. Twenty rectangular alumina plates* of known average strength were broken prior to each test to check instrument** calibration and knife edge alignment and again after breaking the test specimens to check for any drift in the testing machine. The MOR of the test specimens was calculated from the equation for cylindrical rods

$$MOR = \frac{8PL}{\pi D^3} \qquad (3)$$

Where P is the applied load, L the knife edge span (21.5 mm) and D the rod diameter.

---

 * AlSiMag 614 Technical Ceramics, 3M Corp, Minneapolis, MN.
** Instron Corp, Canton, MA.

E. SEM and AES

The fracture and external surfaces of randomly selected specimens were coated with ∿20 nm of gold-palladium and examined with a scanning electron micro-scope* (SEM) equipped with an energy dispersive X-ray analyser interfaced to a computer** for qualitative and quantitative elemental analysis. Surface chemical compositions were measured in ultra-high vacuum with a scanning Auger microscope.*** Relative atomic concentration of Ca and Si were determined using the ratio of the peak-to-peak signal height for each element to that for oxygen. The electron beam was operated in a defocused mode to analyse an area of ∿200 μm^2. In depth analysis was achieved by sputtering the surface at an estimated rate of 1.7 nm/min using an Ar ion gun operated at 2 KV.

F. Analysis of Aging Liquids

The aging liquids were analysed for Ca, Si, Al, and Na by atomic absorption spectrophotometry[†] (AAS). When no dilution was needed, the liquids were aspirated directly into the burner chamber from their container. No lanthanide solution was needed since the interference due to ionization was negligible. Standard solutions and blanks

---

  * JSM-35CF, JEOL Corp., Peabody, MA.
 ** KEVEX Corp., Foster City, CA.
*** Physical Electronics Inds., Eden Prairie, MN.
  † Model 560, Perkin-Elmer, Norwalk, Conn.

were inserted at regular intervals to check for instrument drift and calibration.

G. X-ray Diffraction

An X-ray diffractometer[††] and Debye-Scherrer camera were used to identify the crystalline phases present inside or on the external surface of a specimen before and after aging. Finely powdered samples were packed into a thin-wall (0.01 mm) low absorbance glass capillary tube 0.5 mm in diameter which was rotated in the camera during exposure.

[††] XRD-5, General Electric Co., Schenectady, NY.

III. RESULTS

A. Static Fatigue

The time to failure data for the three aluminas tested in demineralized water and loaded at 75% of their respective dry average failure load (AFL) are plotted in Fig. 1 and recorded in Appendix A. Instant failures were included in the calculation of the fraction of specimens surviving. The time to failure of each alumina was found to be temperature dependent with specimens tested at 70°C having more instantaneous failures and shorter total failure times. Alumina C had the lowest survival rate, followed by alumina B and A. Only one of the 16 alumina C specimens tested at 70°C survived longer than 10s. Alumina A showed the smallest static fatigue, 62% surviving the 14 day test period in demineralized water at 37°C and 19% surviving at 70°C. The 50% failure time of the aluminas listed in Table II were taken from the curves in Fig. 1.

Using the Chi-square test suggested by Mantel and Haenszel[34] for comparing two survival distributions, the survival patterns of the 3 aluminas were significantly different at the 99% confidence level. The difference between the 37° and 70°C data for the aluminas A and B were significant at the 95% confidence level.

The reduction in the time to failure with increasing load for alumina C at 37°C in demineralized water is evident from Fig. 2. Only one alumina C specimen broke at 37°C within 14 days at 55% AFL while at 75% AFL all specimens had failed in about 1 h. At 37°C, total instant failure occurred for alumina A loaded at 90% AFL and for alumina B at 80% AFL. Aluminas A and B were not tested below 75% AFL.

The time to failure data for each alumina tested at 37°C using 75% AFL are shown as Weibull probability plots in Fig. 3. The data points for alumina C fit a straight line reasonably well. The fit for aluminas A and B is poorer, but the scatter in the points does not overlap. Assuming that each data set belongs to a Weibull distribution, the shape and scale parameters were estimated.[35] The survival probability of the aluminas calculated from these parameters are listed in Table III, and the large differences at periods >1 h agree with the results in Fig. 1.

B. Flexural Strength

The flexural strength reduction, expressed as a percentage of the dry strength, of each alumina after 7 days in 0 to 8 wt % HF solution is shown in Fig. 4. All three aluminas were weaker after aging (no load) 7 days in demineralized water, but the reduction for alumina A was small. Fahr et al[32] also found alumina B specimens showing larger flexural strength reduction than alumina A specimens aged in demineralized water at 37°C up to 52 weeks.

In these HF solutions, the two implant grade aluminas A and B, were substantially stronger than alumina C. Their flexural strength at 37°C was nearly independent of HF concentration, but the flexural strength of alumina C was substantially lower ($\sim$90%) after 7 days in 8 wt % HF at 70°C. The number of specimens tested and the statistical significance of the strength compared with the dry or wet strength at 37°C are listed in Table IV. Also included, are the data for aluminas A and B aged at 70°C which are not shown in Fig. 4. Generally, the aluminas aged at higher temperature (70°C) were weaker than those aged at 37°C.

C. Aging Liquids

Demineralized water in contact with the aluminas at 37°C showed rapid increase in Ca concentration after 3 h and reached a maximum after $\sim$30 h, as shown in Fig. 5. The measured Ca concentration has been corrected for the surface area of the specimens. The water in contact with alumina B contained the most Ca followed by aluminas C and A, in agreement with other investigators[32] who found more Ca dissolved from alumina B (0.30 ppm) than alumina A (0.06 ppm) in 3 weeks by demineralized water at 37°C. The Ca concentration of demineralized water aged identically in the plastic container (blank sample) was the same as the starting demineralized water, showing that no contamination occurred during aging.

Al was undetectable in the water after aging, in agreement with Avigdor et al[5], who detected no Al in the water

used for static fatigue testing of a high purity*, porous alumina of 65.1% theoretical density. Österholm et al[18] also did not find Al in deionized water in contact with a 96% Al_2O_3 alumina** powder for 21 days at 40°C. Si and Na were also undetectable in the demineralized water after aging. The lower sensitivity and higher noise level of the instrument for Si and Na made their detection more difficult than for Ca or Al.

The amount of Ca found in the demineralized water did not change significantly when a specimen was under load during aging, as shown in Fig. 5. The alumina A specimens were aged at 75% AFL for 290 h at 37°C along with 5 unstressed samples. The average Ca concentration of the water was 0.035 ± 0.01 and 0.039 ± 0.01 ppm/cm^2 for the stressed and unstressed samples, respectively. This difference is statistically insignificant. Similarly, the Ca concentration of the water containing aluminas B and C loaded at 65% AFL were not significantly higher than the water containing unstressed samples.

The concentration of elements in the HF solutions was quite different from that of demineralized water. After being in contact with the aluminas for 7 days at 37°C, the Ca concentration was less than in water and decreased with

---

* Made from Alcoa A-14, ALCOA, Pittsburgh, PA.
** AlSiMag 614, 3M Corp., Minneapolis, MN.

increasing HF concentration as shown in Fig. 6(A). The
decrease in Ca is probably due to the precipitation of
CaF_2 crystals, which were detected by XRD on the external
surface of alumina C aged 7 days in 8 wt % HF at 37°C.
In contrast, the Si and Al concentration of the HF solutions
was 10-1000 times higher (Fig. 6(B)) than the Ca concen-
tration and tended to increase slightly with increasing
HF concentration. The HF acid most probably enhanced the
dissolution of the impurity containing phase(s). Yamada
et al[40] found 0.137 wt % Al_2O_3 and 0.0009 wt % SiO_2 in
solution after boiling a high purity alumina* in 5% HCl
for 2 h.

The most Al was dissolved from alumina C, followed
by alumina B and alumina A. The most Si in solution also
occurred for alumina C followed by alumina A and alumina B.
Despite the relatively large amount of Si in the HF solutions,
calculations using the SiO_2 concentrations in Table I,
show that the concentration of Si in solution is smaller
than if all the SiO_2 in each alumina specimen had been
totally dissolved. The presence of trace amounts of Na
in the HF solutions in contact with alumina C was indicated
by the appearance of the characteristic yellow flame during
solution analysis, but the Na concentration was below the
instrument detection limit.

---

* Made from A-16SG powder, ALCOA, Pittsburgh, PA.

D. Ca and Si Distribution

AES of the as-washed external surface prior to aging showed that alumina B contained the most Ca, followed by aluminas C and A (Fig. 7(A)), which is the same order as the Ca concentration found in demineralized water, Fig. 4. The Ca-rich layer on the external surface of alumina A was thinner (<45 nm) than that on the external surface of aluminas B and C, which extended beyond the estimated ∿45 nm depth removed by sputtering. Ca was undetectable on the external surface of alumina A and there was much less Ca on the external surface of aluminas B and C after aging for 7 days at 37°C in demineralized water, see Fig. 7(A). Ca reduction from the external surface of aluminas A and B were also observed by other investigators[32] after aging 3 weeks in demineralized water at 37°C (Table V) and aging in vivo (implanted in rats) up to 52 weeks.

Fig. 7(B) shows the Ca present on the fracture surface of as-received specimens. Ca was again undetectable on the fracture surface of alumina A. Unlike the external surface, more Ca was present on the fracture surface of alumina C than in alumina B, and was segregated mainly at the grain boundaries. The AES data from the present study are in reasonably good agreement with published data[16,28,32], as seen in Fig. 7(A), 7(B), and Table V. The few discrepancies could be due to manufacturing variables such as different

raw materials and firing procedures, or to small differences in the AES measurements.

Si was also present on the external surface of the three as-washed aluminas, especially aluminas A and B, where a thin ($\sim$4 nm) Si-rich layer was found (Fig. 8). In depth analysis showed that alumina B had the highest Si content from slightly below the surface to >45 nm into the bulk. The amount of Si in aluminas A and C was about the same at depths of $\sim$10 nm or more below the surface. The Si concentration on the external surface, after aging in water, of alumina A and B was greatly reduced, but was slightly higher on alumina C. Si was undetectable on the fracture surface of aluminas A and B. Si was found only on the fracture surface of alumina C at about the same concentration as at the external surface.

E. Microstructure

Scanning electron micrographs of the as-washed external surface in Figs. 9(A), 9(B), and 9(C), show that the three aluminas had dissimilar surface morphology. The external surface of alumina A, Fig. 9(A), was covered by patches of partially sintered grains. The uncovered areas appearing rather smooth. The grains on the external surface of alumina B, Fig. 9(B), were rounded and the lines on some of the grains suggest some type of thermal treatment. The external surface of alumina C was rough. Visible cracks and broken grains suggest the surface of alumina C had been ground after firing (Fig. 9(C)).

In alumina A (Fig. 9(D)) and alumina C (Fig. 9(F)),
the fracture was primarily transgranular with a small
amount of intergranular cracking. Intergranular fracture
was predominant in alumina B, as shown in Fig. 9(E).

No second phase was detected at the fracture surface
of aluminas A and B. Phase(s) containing significantly
more Ca and Si (Figs. 10(C) and 10(F)) than the bulk were
observed occasionally, however, in alumina C at grain boundary
junctions (Figs. 10(A), 10(B), and 10(D)). Fig. 10(C)
shows the X-ray spectrum of the second phase superimposed
on that of the bulk. The higher concentration of Si
and Ca in the second phase is clearly evident. A grain
boundary phase in this commercial alumina has been reported
by Petrovic and Stout[36] using transmission electron micro-
scopy, but they did not state whether the phase was glassy
or crystalline, or present its composition.

Microstructural examination of the external and fracture
surfaces of the three aluminas showed no difference between
specimens that broke at widely different times during the
static fatigue measurements, or between as-washed specimens
and those aged in water. Careful examination across the
fracture surface and along the broken edges revealed no
distinct region of slow crack growth or any unusual features
around possible fracture origins.

There was no detectable microstructural change in
alumina A after aging in the HF solutions, but new features

appeared in a few alumina B specimens and in nearly all
the alumina C specimens. Circular patterns or rings were
visible on the fracture surface of alumina B aged 7 days
in 8 wt % HF at 70°C (Fig. 11(A)) and alumina C aged in
2 and 4 wt % HF at 37°C (Figs. 12(A) and 12(B)). These
rings were undetected in alumina A and visible in only
a few alumina B specimens. In alumina C, the rings were
highly visible in most of the samples aged 7 days in 2-4
wt % HF. The width of the outer ring depended mainly on
the HF concentration and was less dependent on aging
temperature and time. Alumina C specimens aged in 8 wt %
HF did not generally show these ring patterns, but the change
in microstructure characteristics and ∿90% reduction in
flexural strength were stong evidence that the HF solution
had completely penetrated the ∿3 mm diameter rods. The outer
colored ring in Fig. 12(C) also shows the penetration of the
dye into alumina C after 7 days in 8 wt % HF at 37°C.

SEM examination of the outer ring portion of alumina C
showed that the fracture mode was completely intergranular,
and rod-like crystals were present in some of the pores and
voids between the grains, Fig.s 12(E) and 12(F). The X-ray
signal from these small crystals was weak due to their small
size and its absorption by the surrounding grains, but they
were found to contain slightly more Ca than the bulk, as
shown in Fig. 12(G). The X-ray spectrum of the bulk always
showed only Al. The fracture mode in the unattacked center

of the specimen (Fig. 12(D)) was primarily transgranular and the fracture surface appeared smooth, as if the crack front had been propagated across a single plane. No new crystals were found in the central region.

Clusters of plate-like crystals, containing Ca and Al, were observed on the external surface of alumina C after 7 days in 2 wt % (Fig. 13(A)) and in 8 wt % HF (Fig. 13(C)) at 37°C. In only a few cases was Si ($\sim$20 wt %) detected in these plate-like crystals, and there was no direct correlation between the type of crystal formed and the detected Si content. If the Al signal shown in Fig. 13(D) came exclusively from these crystals and not from the underlying alumina, then its intensity indicates that the crystal contain approximately equal weights of Ca and Al. These crystal clusters contain more than one type of crystal, as is evident from the smaller regularly shaped crystals shown in Fig. 13(E). X-ray powder diffraction of these clusters showed the presence of CaF_2, a small amount of α-Al_2O_3, and unidentified phase(s). The d-spacings and intensity of the diffraction peaks are listed in Appendix B.

No new crystals were found on the surface of the alumina B specimens after aging in HF solutions. Some specimens aged in 8 wt % HF had a faint circular ring (Fig. 11(A)) on their fracture surface. The microstructure of both the center (Fig. 11(B)) and the ring (Fig. 11(C))

of the specimen was identical to that of as-washed specimens. Comparison of the external surface of an as-washed specimen (Fig. 11(D)) with one aged in 8 wt % HF at 70°C for 14 days (Fig. 11(E)) showed that some etching had occurred and the grain boundaries were cracked or heavily grooved. The X-ray spectrum in Fig. 11(F) shows a slightly higher concentration of Si than spectra representing the external surface of as-washed specimens.

Other investigators who exposed these aluminas to saturated steam at 266°C found extensive crystal growth on the external surface of aluminas A and B[32] after 25 days and on alumina C[29] after 6 days. Some small particles were also observed[32] on the external surface of alumina B aged in vivo (rats) although energy dispersive X-ray analysis showed only Al.

IV. DISCUSSION

The dissolution of the Ca containing phase(s) by demineralized water is a likely explanation for the difference in the static fatigue, measured as time to failure, of the three aluminas investigated in this study. Clearly, Ca is dissolved from each alumina when immersed in demineralized water at 37°C, as is evident from the increase in Ca concentration of the water (Fig. 5), and from the decrease in Ca concentration at the external surface (Fig. 7(A)) of each alumina after immersion. Time to failure in water of the two orthopedic aluminas A and B appears to be related to the amount of Ca found in solution. Alumina A shows the smallest static fatigue as indicated by the longest time to failure in Fig. 1 as well as the lowest Ca dissolved in water (Fig. 5).

The correlation between static fatigue and Ca in solution is less clear when the non-orthopedic grade alumina C is included. It showed the highest static fatigue among the three aluminas although the Ca in solution was intermediate between aluminas A and B. Possible explanations for this discrepancy for alumina C are discussed later.

It is important to note that the static fatigue of all three aluminas correlates well with the Ca concentration

found on the fracture surface of each alumina, which is less likely to be affected by any post-firing processing of the aluminas. It is evident from a comparison of Figs. 1 and 7(B) that alumina A had the smallest static fatigue and lowest Ca concentration (undetectable) on the fracture surface. Similarly, alumia B had an intermediate static fatigue and Ca concentration while alumina C showed the highest static fatigue and highest Ca concentration on its fracture surface. The larger proportion of transgranular fracture in alumina A could lower the amount of Ca detected on the fracture surface, although the proportion of transgranular failure is not too large to change the correlation.

The dissolution of the Ca containing phase(s) from the external surface and grain boundaries of these aluminas would be expected to reduce the intergranular bonding and could lead to microcracks (crack formation, extension, or crack tip sharpening) close to the external surface. The microcracks could increase the susceptibility of these aluminas to static fatigue. No evidence of such a weakening process was found in any of the aluminas after immersion in water probably because of the small amount of the dissolution. The penetration of the aluminas by the HF solutions and the dissolution of the grain boundary phase(s) by HF was clearly evident, however, in alumina C and a few specimens of alumina B. Chemical attack of the Ca containing phase(s), similar

to that by HF solution, could also have occurred when the aluminas were immersed in demineralized water, but to a much lower degree.

The weakening of an alumina by dissolution of the Ca containing phase(s), most likely a glassy phase, can also account for the temperature dependence of static fatigue, seen in Fig. 1, since most glasses become more soluble at higher temperatures. The data listed in Appendix C for a few exploratory tests shows that significantly more Ca was dissolved from alumina B at 70°C than at 37°C, which correspond to its shorter time to failure at 70°C. The rate of reaction of $CaO \cdot Al_2O_3 \cdot SiO_2$ glasses with HF solutions has been reported[37] to increase with increasing temperature which could account for the lower flexural strength of the aluminas aged in the HF solutions at 70°C.

There are several factors regarding the Ca containing phase in these aluminas which could affect the amount of Ca in solution and, therefore, the correlation with static fatigue. This is particulary true for alumina C. Differences in the chemical composition of the calcium-aluminosilicate glassy phase in these aluminas could be a factor of major importance since their solubility in water of HF solutions can be expected to be highly dependent upon their composition. Second, the distribution and quantity of the glassy phase is important. A lower proportion of Ca at the external

surface of a specimen should result in less Ca being
found in solution if all these factors are equal. Such
a correlation can be seen between the AAS analysis of the
water and the Ca concentration at the external surface in
Figs. 5 and 7(A). The post-firing surface grinding of alumina C,
as indicated by the cracked and broken grains on the external
surface in Fig. 9(C), could have removed much of the Ca-
rich layer on this alumina, thereby accounting for the
low concentration of Ca found in solution, Fig. 5. The
higher Ca concentration shown in Fig. 7(A) for a polished
surface of an alumina C specimen[28] demonstrates the possi-
bility of removing the external Ca by machining.

A third factor affecting the correlation between the
static fatigue and Ca in solution, particularly for alumina
C, is the difference between its wet and dry strength. The
wet strength of alumina C was 16% lower than its dry
strength, see Fig. 4 or Table IV, while aluminas A and B
had a difference of 7 and 13%, respectively. Since the
static fatigue specimens were loaded to 75% dry AFL in
demineralized water, the lower wet strength of alumina C
could partially account for its shorter time to failure
because it would be loaded at ∿89% of its effective (wet)
strength during the static fatigue experiment. However,
the large difference in the time to failure of the aluminas
can not be entirely due to the difference in their wet and
dry strength. Comparison of the 75% AFL failure curve of

alumina A (Fig. 1) with that of alumina C loaded at 65% AFL (Fig. 2) which corresponds to ∿80% and ∿77% of wet AFL for aluminas A and C respectively, shows that despite a smaller number of instant failures, alumina C still has shorter complete failure time.

The Ca containing phase at the grain boundaries of these aluminas is probably a glass, based on the known glass-forming tendency of $CaO \cdot Al_2O_3 \cdot SiO_2$ compositions, the absence of XRD evidence for a Ca and Si containing crystalline phase, and the fluid-like appearence of the grain boundary phase in alumina C (Figs. 10(A), 10(B), 10(D)). Furthermore, a glass phase has been observed[38] and is believed to be the Ca containing phase[20] in a 96% Al_2O_3* dense alumina. Using transmission electron microscopy, Hansen and Philips[39] also observed a continuous Ca containing amorphous phase in a high purity commercial alumina**.

The composition of the intergranular glassy phase in the three aluminas investigated can not be determined accurately, but rough estimates can be made using the available AES and AAS analysis data. The Ca and Si concentration at the fracture surface of these aluminas, seen in Figs. 7(B) and 8, and Table V, provide a reasonable estimate of the Ca/Si ratio of the grain boundary phase.

----

 * AlSiMag 614, 3M Corp., Minneapolis, MN.
** McDanel Refractory Co., Beaver Falls, PA.

The proportion of Al in the second phase can not be determined by AES due to interference of the Al signal from the alumina substrate (the bulk). However the Al and Si concentration of the HF solutions in contact with the aluminas, Fig. 6(B), could be used to calculate the proportion of Al and Si in the glassy phase, assuming that only the grain boundary glassy phase is dissolved by the HF. Combining the Ca/Si and Al/Si ratios give the proportion of these three major components in this phase. Possible complications such as difference in dissolution rate of Si and Al in HF, and the uncertainty in calculating the atomic percent of Ca and Si using the Ca/O and Si/O peak ratios are disregarded. It is not possible to use the Ca concentration in HF solution, seen in Fig. 6(A), because the precipitation of CaF_2 crystals reduces the Ca concentration.

The composition of the grain boundary phase in alumina A is estimated as $nCaO \cdot Al_2O_3 \cdot 5SiO_2$, and in alumina B as $nCaO \cdot 4Al_2O_3 \cdot SiO_2$, where $n > 5$ and not necessarily equal in both cases. The phase dissolved from alumina C by dilute HF acid is estimated as $4CaO \cdot Al_2O_3 \cdot 4SiO_2$, plus a small unknown quantity of Na_2O. The low SiO_2 content calculated for the grain boundary phase in alumina B casts doubt upon it being present as a glass, despite other indications that the phase is glassy. Although all of the Si and Al

dissolved in HF solution has been attributed to a single phase, there could be more than one phase undergoing dissolution. In fact, it is uncertain whether more than one grain boundary phase is present in aluminas A and C. In the two orthopedic aluminas A and B, the grain boundary phase with the higher CaO/SiO_2 ratio is associated with the higher solubility.

V. CONCLUSION

Ca dissolves from high purity, dense, implant grade aluminas within 3 h of immersion in demineralized water at 37°C. This Ca is initially segregated at the grain boundaries and external surface. Dissolution of the grain boundary Ca-rich phase, most probably a calcium-aluminosilicate glass of unknown composition, appears at least partially responsible for the static fatigue of these aluminas. A good correlation was found between the static fatigue in water and the Ca concentration at the grain boundaries or fracture surfaces. The time to failure decreases with increasing Ca concentration. The composition, distribution, and nature (glassy or crystalline) of the grain boundary phase(s) should affect their solubility, and consequently the mechanical properties of the aluminas. The effect of microstructure on static fatigue appears to be minor, since the two orthopedic aluminas has similar grain size (2 μm and 4 μm) and porosity, but had significantly different times to failure. Although the two orthopedic aluminas and the commercial 99% dense alumina had similar chemical compositions and physical properties, large differences in static fatigue and flexural strength after aging in demineralized water and HF solution were observed.

The results of the present study indicate that long term service life and minimum static fatigue in wet environments should be favored by an alumina having the lowest Ca concentration at the grain boundaries and showing minimum Ca dissolution, other properties being similar.

REFERENCES

1. G. Heimke and P. Griss, "Ceramic Implant Materials,"
    Med. & Biol. Eng. & Comput., 18 503-510 (1980).

2. L. L. Hench, "Biomaterials," Science, 208 826-831 (1980).

3. A. White, P. Handler, E. Smith; pp627-632, 674-767 in
    Principles of Biochemistry, 3rd Ed., McGraw-Hill Book
    Co., (1964).

4. C. C. Chen and W. J. Knapp, "Fatigue Fracture of an
    Alumina Ceramic at Several Temperatures," pp691-707
    in Fracture Mechanics of Ceramics, Vol. 2. Edited
    by R. C. Bradt, D. P. H. Hasselman, and F. E. Lange,
    Plenum, New York (1974).

5. D. Avigdor and S. D. Brown, "Delayed Failure of a
    Porous Alumina," J. Am. Ceram. Soc., 61 [3-4] 97-99
    (1978).

6. D. A. Krohn and D. P. H. Hasselman, "Static and Cyclic
    Fatigue Behavior of a Polycrystalline Alumina," J. Am.
    Ceram. Soc., 55 [4] 208-211 (1972).

7. J. E. Ritter, Jr. and J. N. Humenik, "Static and
    Dynamic Fatigue of Polycrystalline Alumina," J. Mat.
    Sci., [14] 626-632 (1979).

8. A. G. Evans and S. M. Wiederhorn, "Proof Testing of Ceramic Materials. An Analytical Basis for Failure Prediction," Int. J. Fract., 10 379-392 (1974).

9. S. M. Wiederhorn; pp635-665 in Ceramics for High Performance Applications. Edited by J. J. Burke, A. E. Gorum, and R. N. Katz, Brook Hill, Chestnut Hill, Mass., (1974).

10. J. E. Ritter, Jr., "Engineering Design and Fatigue Failure of Brittle Materials;" pp667-686 in Fracture Mechanics of Ceramics, Vol. 4. Edited by R. C. Bradt, D. P. H. Hasselman, and F. F. Lange, Plenum, New York (1978).

11. W. S. Hillig and R. J. Charles; pp682-705 in High Strength Materials. Edited by V. F. Zackay, Wiley & Sons, New York (1965).

12. K. Jakus, J. E. Ritter, Jr., and J. M. Sullivan, "Dependency of Fatigue Prediction on the Form of the Crack Velocity Equation," J. Am. Ceram. Soc., 64 [6] 372-374 (1981).

13. C. M. Jantzen, D. R. Clarke, P. E. D. Morgan, and A. B. Harker, "Leaching of Polyphase Nuclear Waste Ceramics; Microstructural and Phase Characterization," J. Am. Ceram. Soc., 65 [6] 292-300 (1982).

14. R. J. Charles, "Static Fatigue of Glass I & II," J. App. Phy., 29 [11] 1549-60 (1958).

15. S. M. Wiederhorn, H. Johnson, A. M. Diness, A. H. Heuer, "Fracture of Glass in Vacuum," J. Am. Ceram. Soc., <u>57</u> [8] 336-341 (1974).

16. S. Sinharoy, L. L. Levenson, W. V. Ballard, and D. E. Day, "Surface Segregation of Calcium in Dense Alumina Exposed to Steam and Steam-CO," Am. Ceram. Soc. Bull., <u>57</u> [2] 231-233 (1978).

17. W. V. Ballard and D. E. Day, "Stability of the Refractory-Bond Phases in High Alumina Refractories in Steam-CO Atmosphere," Am. Ceram. Soc. Bull., <u>57</u> [7] 660-666 (1978).

18. H. H. Österholm and D. E. Day, "Dense Alumina Aged in Vivo," J. Biomed. Mat. Res., <u>15</u> 279-288 (1981).

19. S. Sinharoy, L. L. Levenson, and D. E. Day, "Influence of Calcium Migration on the Strength Reduction of Dense Alumina Exposed to Steam," Am. Ceram. Soc. Bull., <u>58</u> [4] 464-466 (1979).

20. D. E. Day, "Reaction of Alumina Ceramics with Saturated Steam," Am. Ceram. Soc. Bull., <u>61</u> [6] 624-626, 631 (1982).

21. A. W. Funkenbusch and D. W. Smith, "Influence of Calcium on the Fracture Strength of Polycrystalline Alumina," Metall. Trans. A., <u>6A</u> [12] 2299-301 (1975).

22. W. C. Johnson and D. F. Stein, "Additive and Impurity Distributions at Grain Boundaries in Sintered Alumina," J. Am. Ceram. Soc., <u>58</u> [11-12] 485-488 (1975).

23. W. C. Johnson, D. F. Stein and R. W. Rice; pp261-275 in Proceedings of the 4th Bolton Landing Conference. Claitors, Baton Rouge, LA , 1975.

24. H. L. Marcus and M. E. Fine, "Grain-Boundary Segregation in MgO-Doped Al_2O_3," J. Am. Ceram. Soc., 55 [11] 568-570 (1972).

25. V. P. Maksimov, "Microprobe Investigations of Impurity and Additive Distribution in Sintered Al_2O_3," Inorg. Mater. (Engl. Transl.), 15 [1] 78-81 (1977).

26. R. J. Jupp, D. F. Stein and D. W. Smith, "Observations on the Effect of Calcium Segregation on the Fracture Behavior of Polycrystalline Alumina," J. Mat. Sci., 15 [1] 96-102 (1980).

27. D. R. Clarke, "Grain-Boundary Segregation in MgO-Doped Al_2O_3," J. Am. Ceram. Soc., 63 [5-6] 339-341 (1980).

28. S. Sinharoy, L. L. Levenson and D. E. Day, "Steam-Enhanced Calcium Segregation in Dense Alumina," J. Vac. Sci. Technol., 16 [2] 503-506 (1979).

29. M. A. Smith, D. E. Day and L. L. Levenson, "Steam-Enhanced Impurity Segregation in Dense Alumina," Am. Ceram. Soc. Bull., 62 [6] 638-641 (1982).

30. R. C. Sundahl, "Relationship Between Substrate Surface Chemistry and Adhesion of Thin Films," J. Vac. Sci. Technol., 9 [1] 181-185 (1972).

31. R. E. Mistler, P. T. Morzenti and D. Shanefield, "Fine Grained Alumina Substrates: II, Properties," Am. Ceram. Soc. Bull., 53 [8] 564-568 (1974).

32. A. Fahr, R. F. Brown and D. E. Day, "In Vivo and In Vitro Aging of Orthopedic Aluminas," to be published in J. Biomed. Mat., Vol. 17 (1983).

33. J. E. Ritter, Jr. and C. L. Sherburne, "Dynamic and Static Fatigue of Silicate Glasses," J. Am. Ceram. Soc., 54 [12] 601-605 (1971).

34. N. Mantel and W. Haenszel, "Statistical Aspects of the Analysis of Data from Retrospective Studies of Disease," J. Nat. Cancer Inst., 22 [4] 719-748 (1959).

35. L. J. Bain, pp264-278 in Statistical Analysis of Reliability and Life-Testing Models, Marcel Dekker Inc., New York (1978).

36. J. J. Petrovic and M. G. Stout, "Fracture of Al_2O_3 in Combined Tension/Torsion: I," J. Am. Ceram. Soc., 64 [11] 656-660 (1981).

37. S. T. Tso and J. A. Pask, "Reaction of Glasses with Hydrofluoric Acid Solution," J. Am. Ceram. Soc., 65 [7] 360-362 (1982).

38. H. Österholm and D. E. Day, "Calcium Migration in Dense Alumina Aged in Water and Physiological Media," Am. Ceram. Soc. Bull., 60 [9] 955-959 (1981).

39. S. C. Hansen and D. S. Philips, "Grain Boundary Micro-
    structure in a Commercial Refractory," Presented at the
    84th Annual Meeting of Am. Ceram. Soc., Abstract in
    Am. Ceram. Soc. Bull., 61 [3] 396 (1982).

40. S. Yamada, N. Kamehara, K. Murakawa, "Improvement in
    As-Fired Surface Finish Resulting From Acid Treatment
    of Prefired Al_2O_3 Substrate," Am. Ceram. Soc. Bull.,
    57 [2] 692 (1978).

TABLE I

Concentration of Major Impurities
and Selected Properties of Aluminas Studied

Alumina	Impurity level (wt %)					Bulk Dens. (g/cm^3)	Calc.** Porosity (vol %)	Mean grain size (µm)	Flexural Strength (MPa)
	CaO	SiO$_2$	Na$_2$O	MgO	Fe$_2$O$_3$				
A*	<0.01	0.02	0.01	0.0	0.01	3.94	1.1	2	520 ± 66[†]
B*	<0.01	0.02	0.01	0.20	<0.01	3.93	1.4	4	481 ± 48
C[ref 28]	0.10	0.80	0.04	0.10	0.10	3.80	4.7	14	333 ± 19
ref 36	0.20	0.40	0.01	0.30	0.06				
ref 29	0.22	0.45							

A Certified implant grade alumina, McDanel Refractory Co., Beaver Falls, PA.

B "Biolox," Feldmühle Akfiengesellschaft, 7310 Plichingen, W. Germany.

C AD-99, Coor's Porcelain Co., Golden, CO.

* Nominal concentration as supplied by manufacturer.

** Using theoretical density of α-Al$_2$O$_3$ as 3.98 g/cm^3.

† Plus or minus values correspond to one standard deviation.

TABLE II

Time for 50% of the Specimens to Fail in
Demineralized Water When Loaded at 75% AFL

Temperature (°C)	Time (s)		
	A	B	C
37	1.2×10^{7} *	250	13
70	1.8×10^{4}	27	0

* Extrapolated

TABLE III

Reliability Approximation (Survival Probability)
of the Aluminas at Selected Time Intervals

Testing Time	Survival Probability		
	A	B	C
1 min	0.93	0.80	0.56
1 h	0.87	0.50	1.27×10^{-3}
1 d	0.80	0.19	0
14 d	0.72	0.03	0
Shape Parameter m	0.152	0.28	0.60
Scale Parameter	1.73×10^9	1.34×10^4	1.52×10^2

TABLE IV

Strength Reduction of Aluminas After Aging 7 Days at Various Conditions

Aging Conds.		Flexural Strength (MPa)	% of dry Strength	Number of Specimens Tested	Significance** 37°C dry Strength	Significance** 37°C wet Strength
			ALUMINA A			
Dry	37°C	519 ± 48*	100	10		
Demin. Water	37	484 ± 77	93	7	Yes (95%)	
	70	514 ± 44	99	5	No	
1% HF	37	463 ± 47	89	12	Yes (99%)	No
	70	441 ± 88	85	15	Yes (99%)	No
2% HF	37	454 ± 53	88	17	Yes (99%)	No
	70	403 ± 51	78	10	Yes (99%)	Yes (95%)
4% HF	37	461 ± 49	89	10	Yes (99%)	No
	70	403 ± 67	78	9	Yes (99%)	Yes (95%)
8% HF	37	463 ± 62	89	5	Yes (99%)	No
	70	379 ± 35	73	7	Yes (99%)	Yes (95%)

* ± values correspond to one standard deviation.

** Student t-test. Number in parenthesis denotes % confidence level.

All strength measurements made with alumina specimens sealed in flexible plastic containers.

TABLE IV (Cont.)

Aging Conditions	Flexural Strength (MPa)	% of dry Strength	Number of Specimens Tested	Significance 37°C dry Strength	Significance 37°C wet Strength
ALUMINA B					
Dry 37°C	443 ± 56	100	5		
Demin water 37	386 ± 25	87	10	Yes (95%)	
70	368 ± 21	83	4	Yes (99%)	Yes (99%)
1% HF 37	387 ± 22	87	12	Yes (95%)	No
70	366 ± 33	83	4	Yes (99%)	Yes (99%)
2% HF 37	399 ± 22	90	9	No	No
70	382 ± 20	86	7	Yes (95%)	No
4% HF 37	381 ± 35	86	10	Yes (95%)	No
70	419 ± 11	95	5	No	No
8% HF 37	377 ± 22	85	7	Yes (95%)	No
70	340 ± 31	77	4	Yes (95%)	Yes (99%)

TABLE IV (Cont.)

Aging Conditions		Flexural Strength (MPa)	% of dry Strength	Number of Specimens Tested	Signigicance 37°C dry Strength	Significance 37°C Wet Strength
			ALUMINA C			
Dry 37°C		308 ± 15		28		
	70	310 ± 20		10		
Demin water	37	260 ± 18	84	26	Yes (99%)	
	70	261 ± 13	85	5	Yes (99%)	No
1% HF	37	190 ± 12	62	15	Yes (99%)	Yes (99%)
	70	127 ± 4	41	5	Yes (99%)	Yes (99%)
2% HF	37	158 ± 8	51	15	Yes (99%)	Yes (99%)
	70	95 ± 11	31	4	Yes (99%)	Yes (99%)
4% HF	37	107 ± 4	32	5	Yes (99%)	Yes (99%)
	70	38 ± 3	12	5	Yes (99%)	Yes (99%)
8% HF	37	75 ± 4	24	5	Yes (99%)	Yes (99%)
	70	30 ± 1	10	5	Yes (99%)	Yes (99%)

TABLE V

Ca/O and Si/O Ratio at External and Fracture* Surface of Aluminas A and B

Aging Conditions	Si/O Ratio $(\times 10^2)$		Ca/O Ratio $(\times 10^2)$		Source
	A	B	A	B	
1 wk sealed inside container at 37°C	11.1(nd)	5.8(nd)	11.2(nd)	4.1(10.4)	Present Study
As received	7.6(<1.0)	5.5(<1.0)	4.0(2.0)	10.0(8.6)	Ref. 32
3 wk in vacuum at 37°C	9.0	6.2	3.8	8.0	Ref. 32
1 wk in demineralized water at 37°C	2.7(nd)	7.5(2.5)	nd(nd)	2.9(0.8)	Present Study
3 wk in demineralized water at 37°C	3.8	4.7	1.8	nd	Ref. 32

nd = not detected

* number in parenthesis

FIGURE CAPTIONS

Fig. 1. Time to failure of aluminas A, B, and
C, in demineralized water at 37° and 70°
C, loaded at 75% average fracture load
(AFL).

Fig. 2. Time to failure of alumina C in demin-
eralized water at 37°C, loaded at 55,
65 and 75% AFL.

Fig. 3. Weibull probability plot of the failure
time for aluminas A, B, and C, using
37°C and 75% AFL data from Fig. 1.

Fig. 4. Reduction in flexural strength of aluminas
A, B, and C, after aging in demineralized
water and HF solution for 7 days. Vertical
lines correspond to plus or minus one
standard deviation.

Fig. 5. Ca concentration of the demineralized water
in contact with aluminas A(O), B(□), and
C(△), at 37°C. Solid symbols represent
alumina A(●) stressed at 75% AFL and
alumina B(■) and C(▲) at 65% AFL while in
water.

Figure Captions (Cont.)

Fig. 6. (A) Ca concentration, and (B) Al (solid
symbols) and Si (open symbols) concentra-
tion of HF solutions in contact with
aluminas A(O), B(□), and C(△), for 7 days
at 37°C.

Fig. 7. Relative Ca concentration of the (A)
external surface and (B) the fracture
surface of as-washed aluminas A(O), B(□),
and C(△), solid symbols (●,■,▲) represent
specimens aged for 7 days at 37°C in
demineralized water. The Ca concentration
of a polished surface (▼) and a fracture
surface (X) of as-received alumina C from
Ref. 28 and 16 are shown for comparison.

Fig. 8. Relative Si concentration at the external
surface of as-washed aluminas A(O), B(□),
and C(△), and (●,■,▲) after they had been
in contact with demineralized water for
7 days at 37°C. Only alumina C(▽) has
detectable Si on the fracture surface.

Fig. 9. Microstructure of the external and fracture
surface of as-washed (A,D) alumina A,
(B,E) alumina B, and (C,F) alumina C.
Bar = 10μm.

Figure Captions (Cont.)

Fig. 10. (A,B,D,E) Appearance of a second
phase at the grain boundary junction
of the fracture surface of as-washed
alumina C specimens, denoted by
arrows. The X-ray spectra in (C) and
(F) correspond to regions denoted by
the larger arrows in (B) and (D)
respectively.

Fig. 11. (A) Fracture surface of alumina B
after aging 7 days in 8 wt % HF at 37°C
showing a faint ring at the outer edge
(denoted by open arrows). (B) A region
in the center and (C) within the outer
ring of the specimen in (A). External
surface of (D) as-washed alumina B and
(E) after aging 14 days in 8 wt % HF at
70°C. The tip of the solid arrows denote
regions of solution attack. The X-ray
spectra of the external surface in (D)
and (E) are compared in (F) where the dots
show the presence of Si in (D).

Figure Captions (Cont.)

Fig. 12. Fracture surface of alumina C

specimens aged 7 days in (A) 2 wt %,

(B) 4 wt %, and (C) 8 wt % HF solution

at 37°C. (C) is an optical micrograph

showing a penetration of dyed HF at

outer surface. (D) Region at the

center of the specimen in (A) (near

the tip of the solid arrow) and (E)

region in the outer ring (tip of open

arrow) show large differences in mor-

phology. (F) shows new rod-like crystal

containing detectable Ca (G) at the

tip of the open arrow in (E).

Fig. 13. External surface of alumina C after aging

7 days at 37°C in (A) 2 wt % and (C,E)

8 wt % HF showing new crystal growths

containing Ca (B,D). The X-ray spectrum

in (B) and (D) correspond to regions

denoted by the solid arrows in (A) and

(E) respectively.
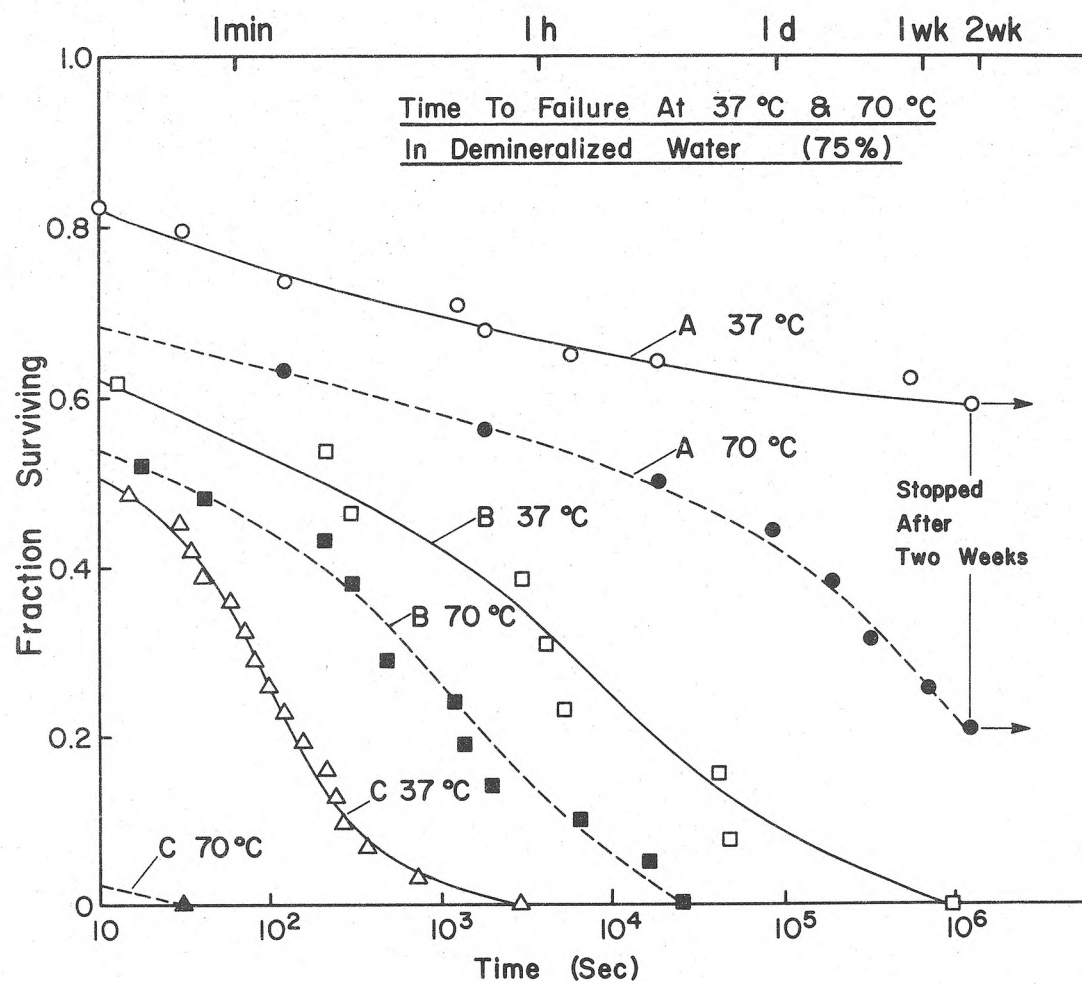
Fig. 1
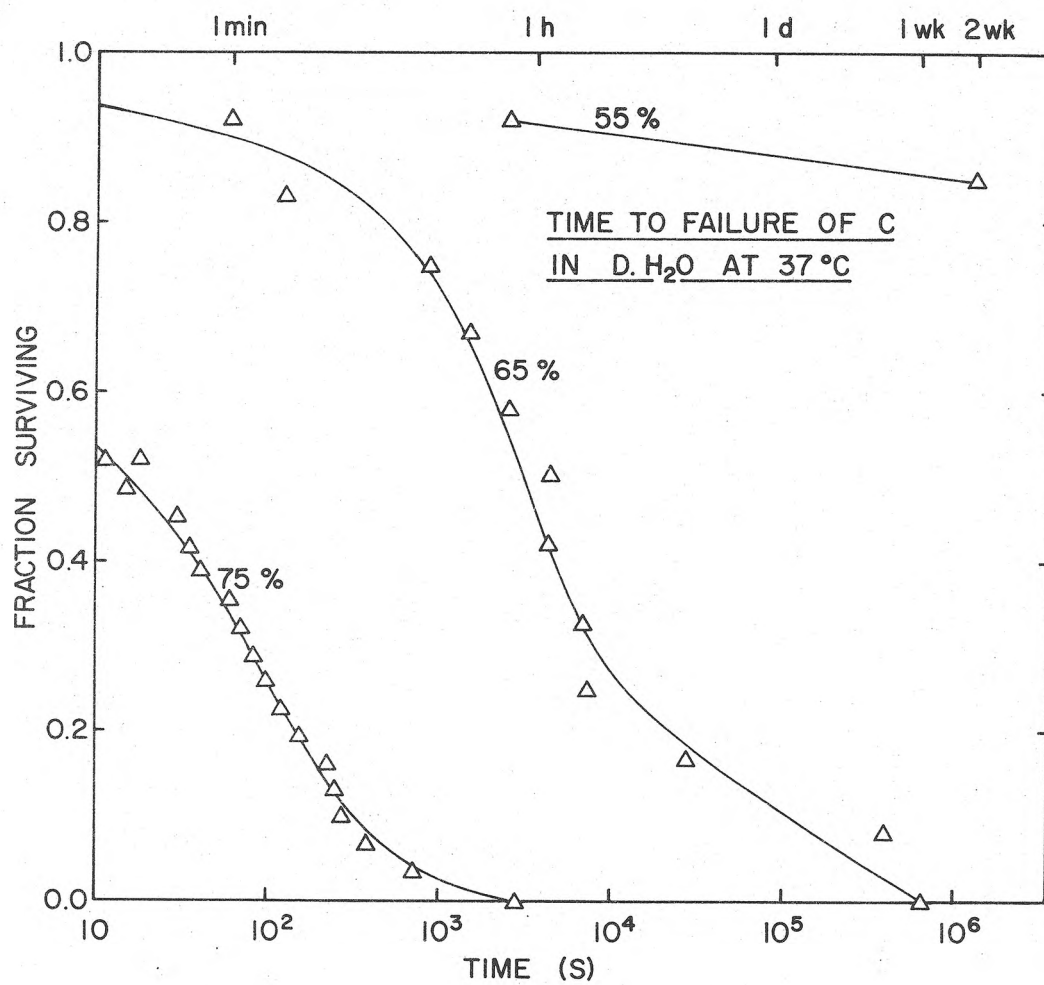
Fig. 2
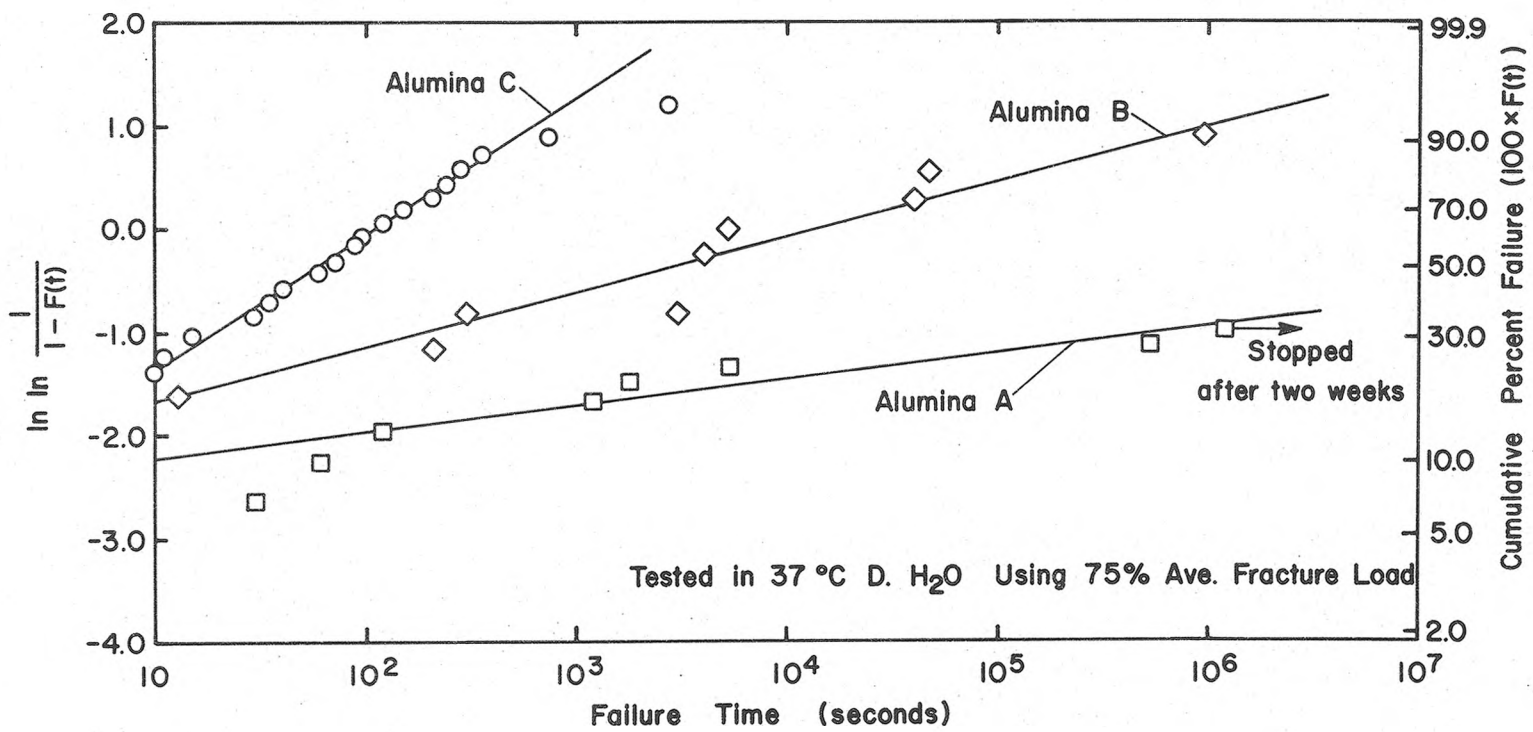
Fig. 3
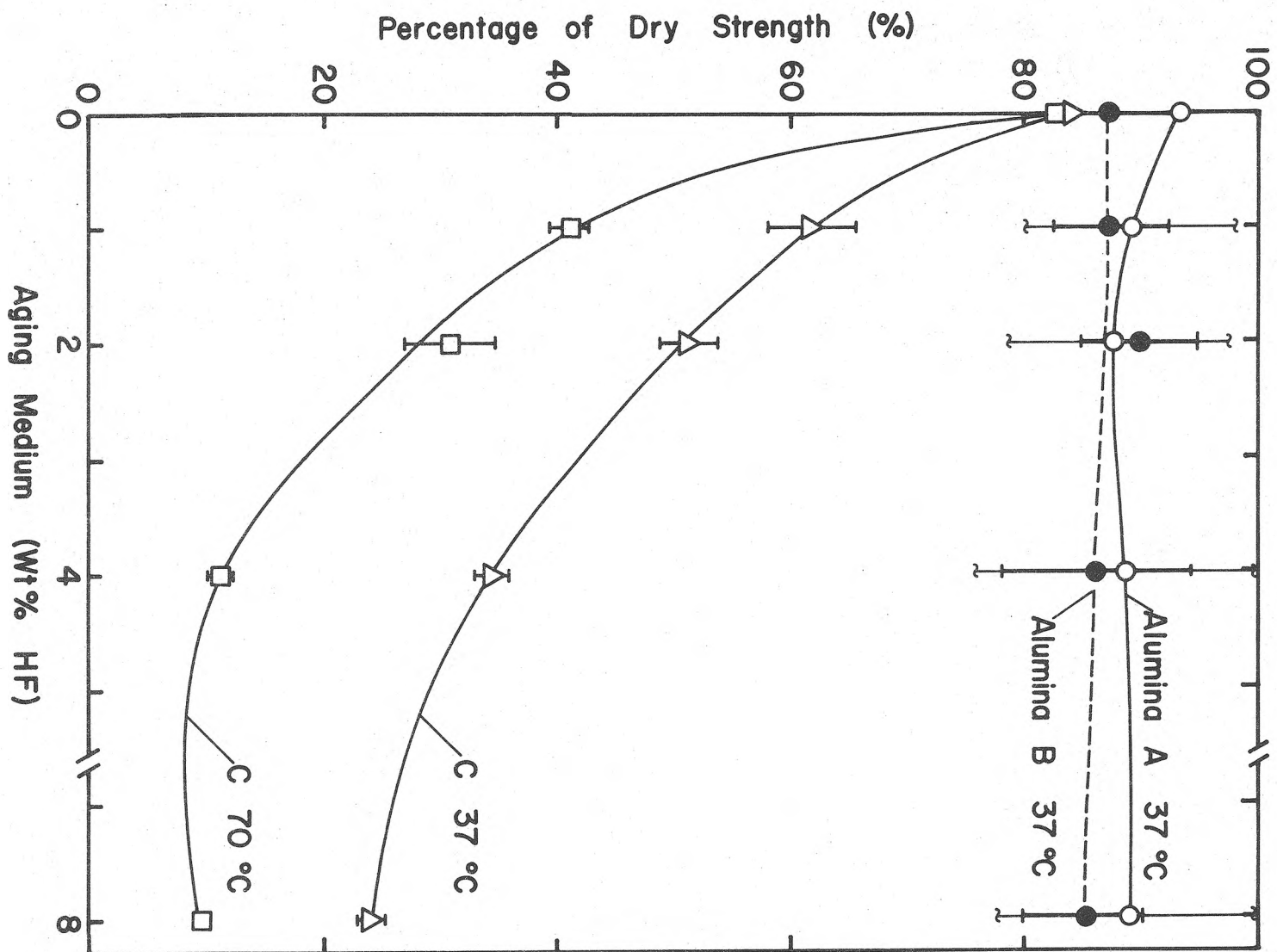
Fig. 4
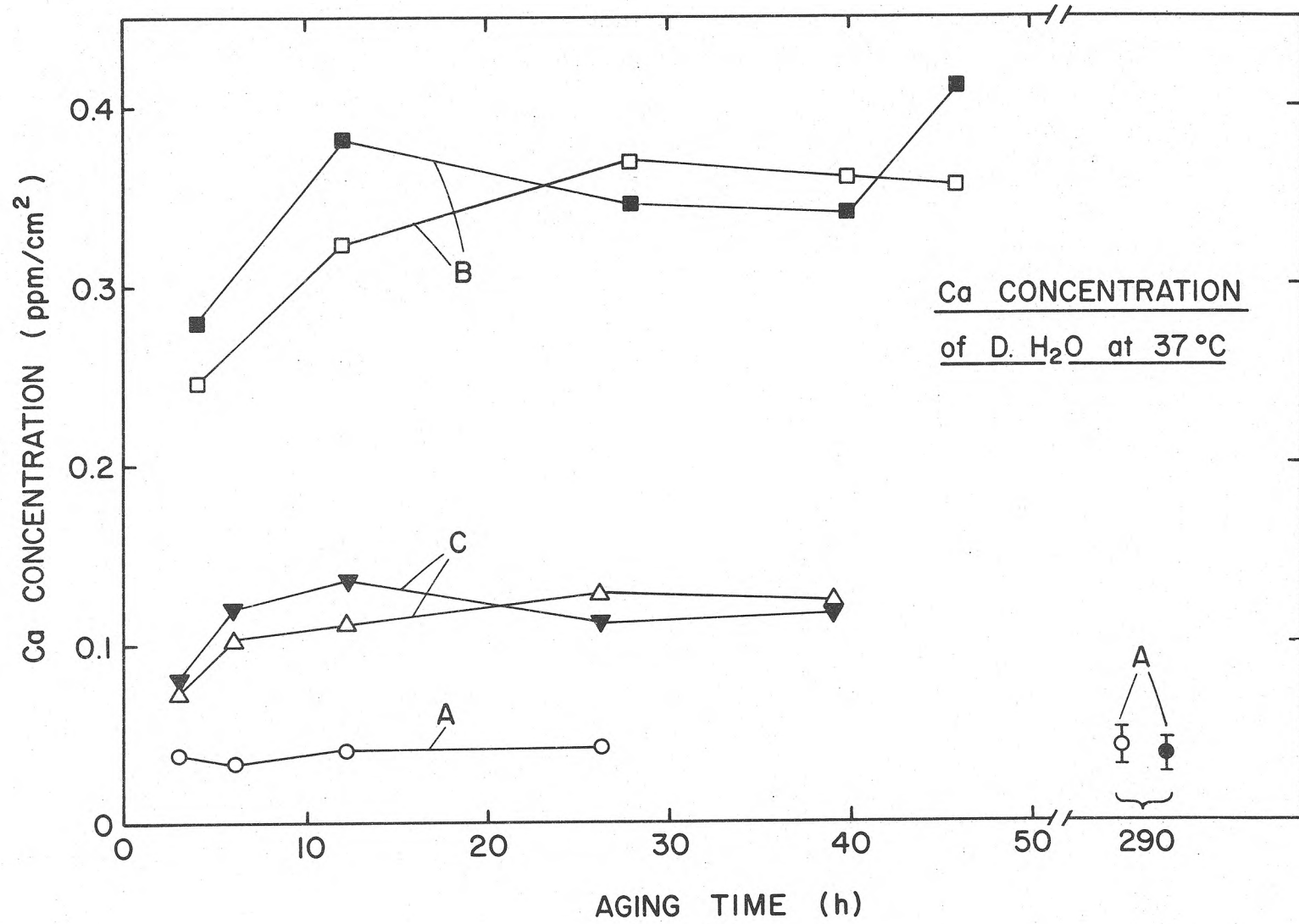
Fig. 5
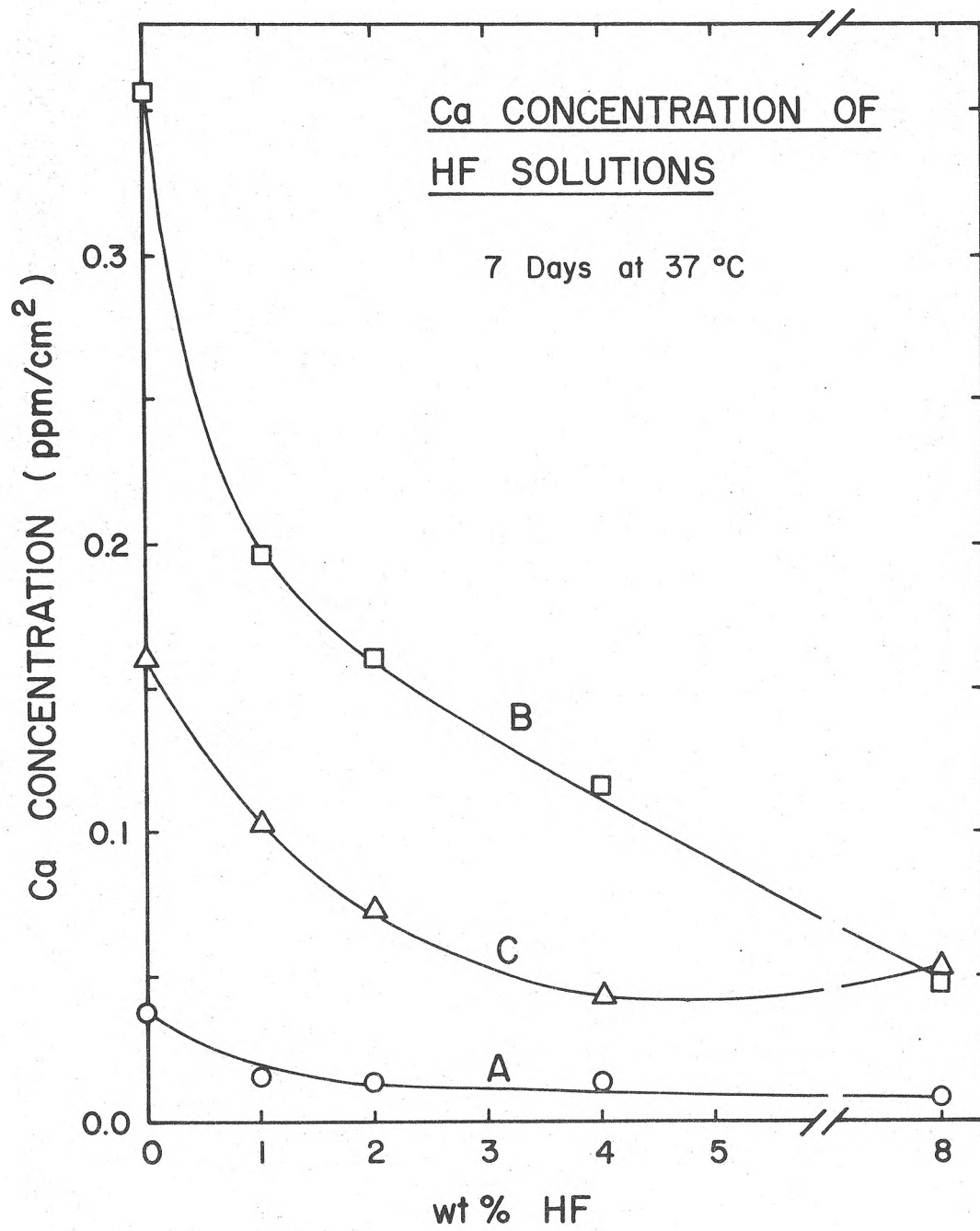
Fig. 6(A)
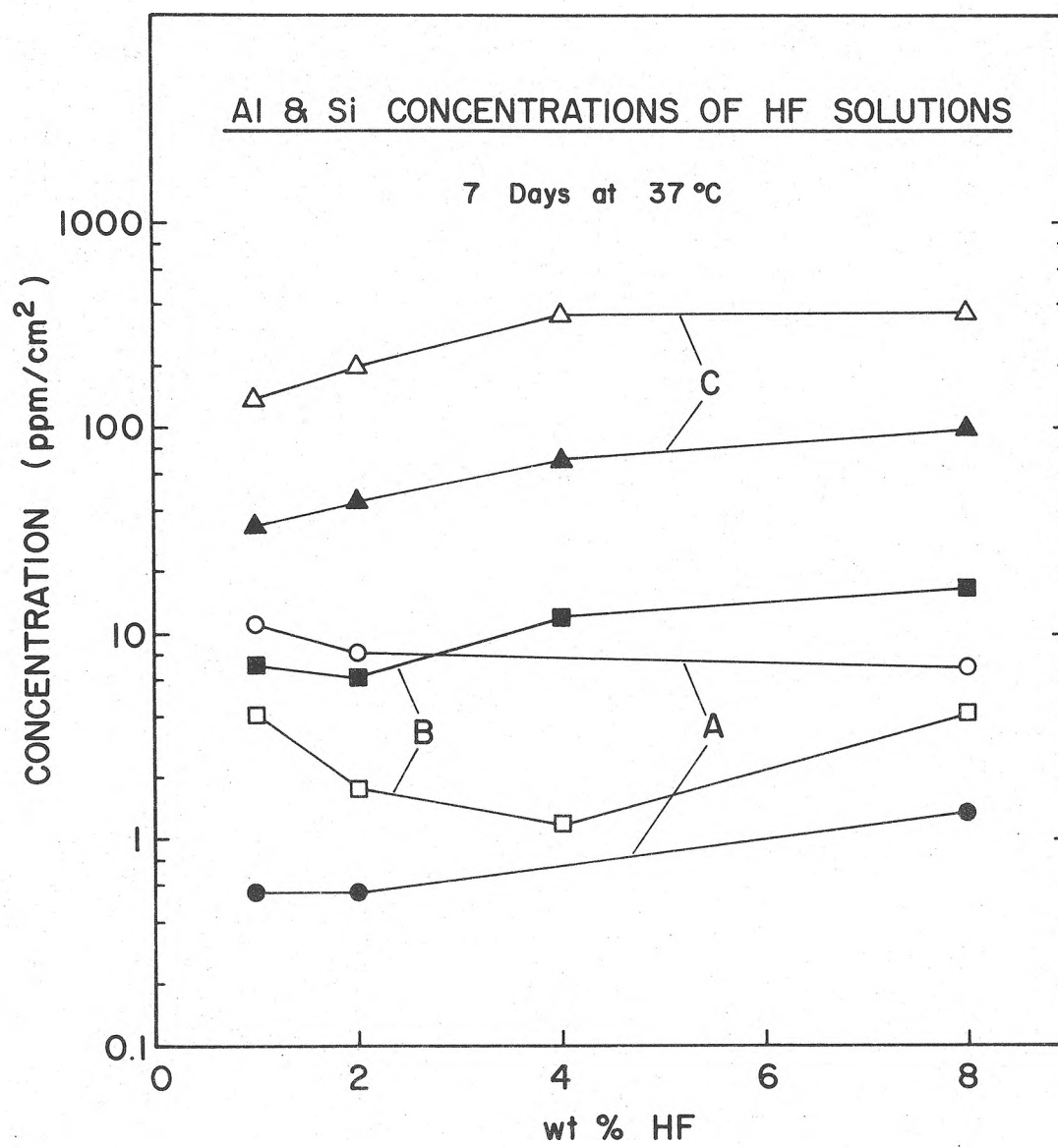
Fig. 6(B)
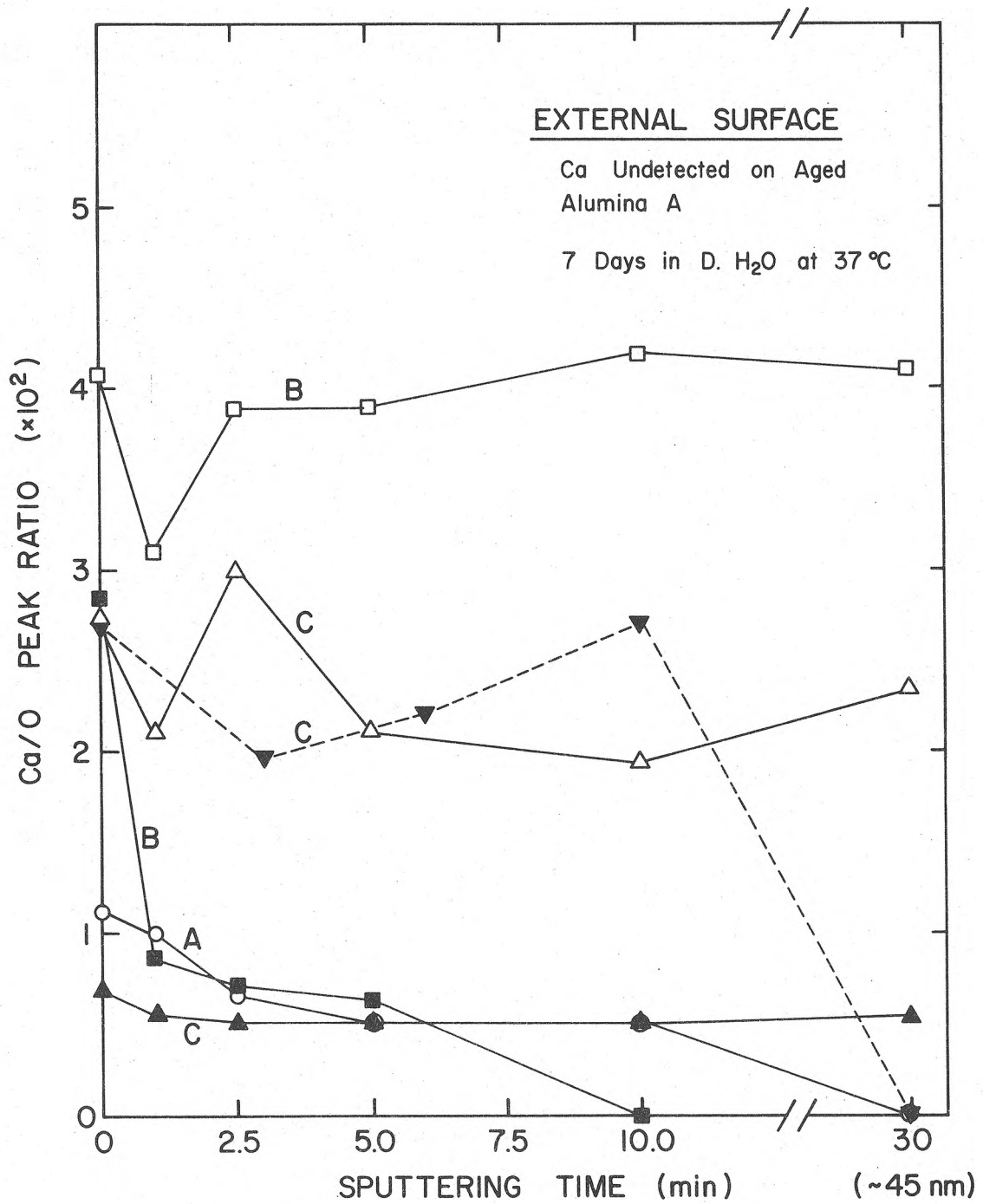
Fig. 7(A)
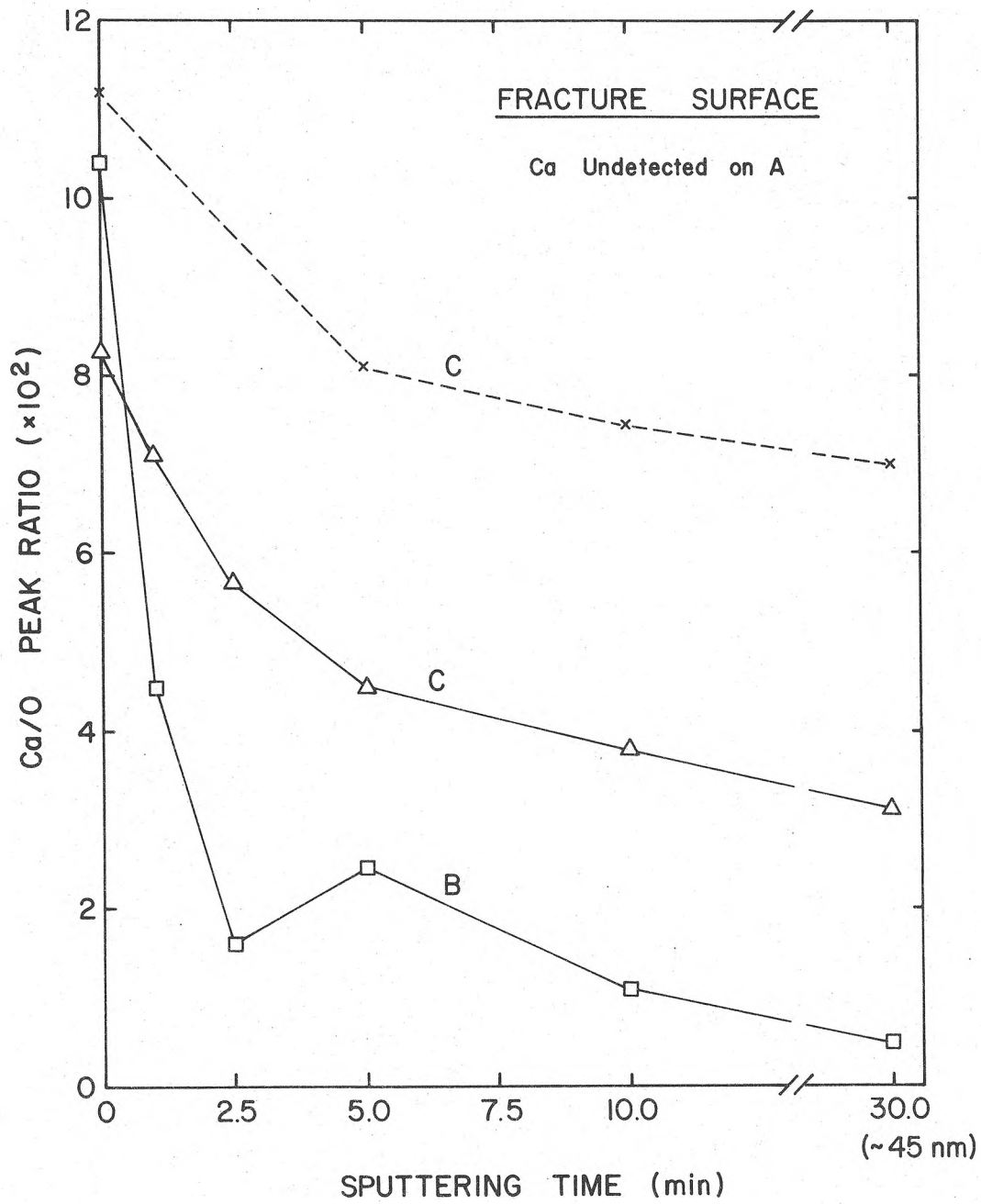
Fig. 7(B)
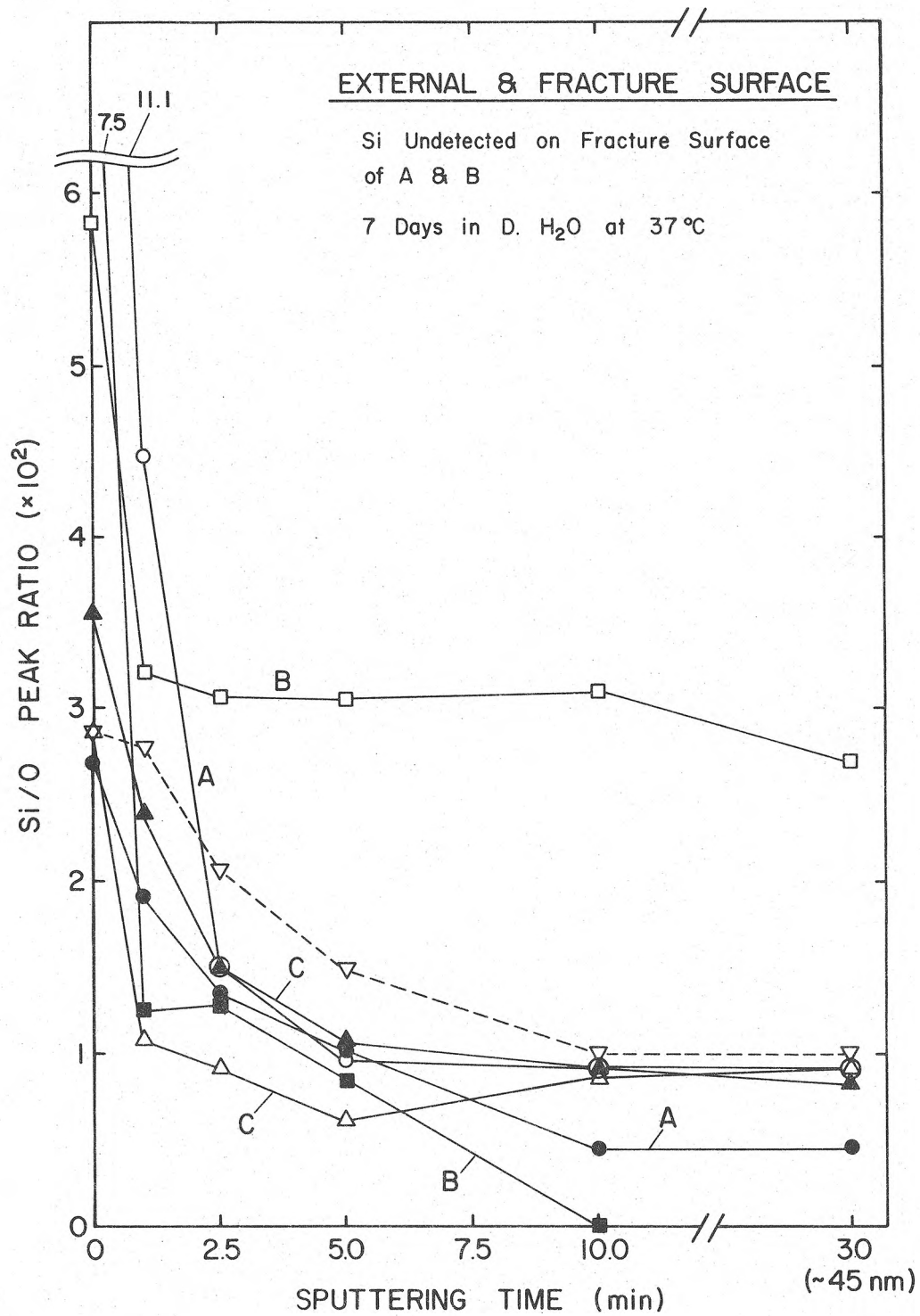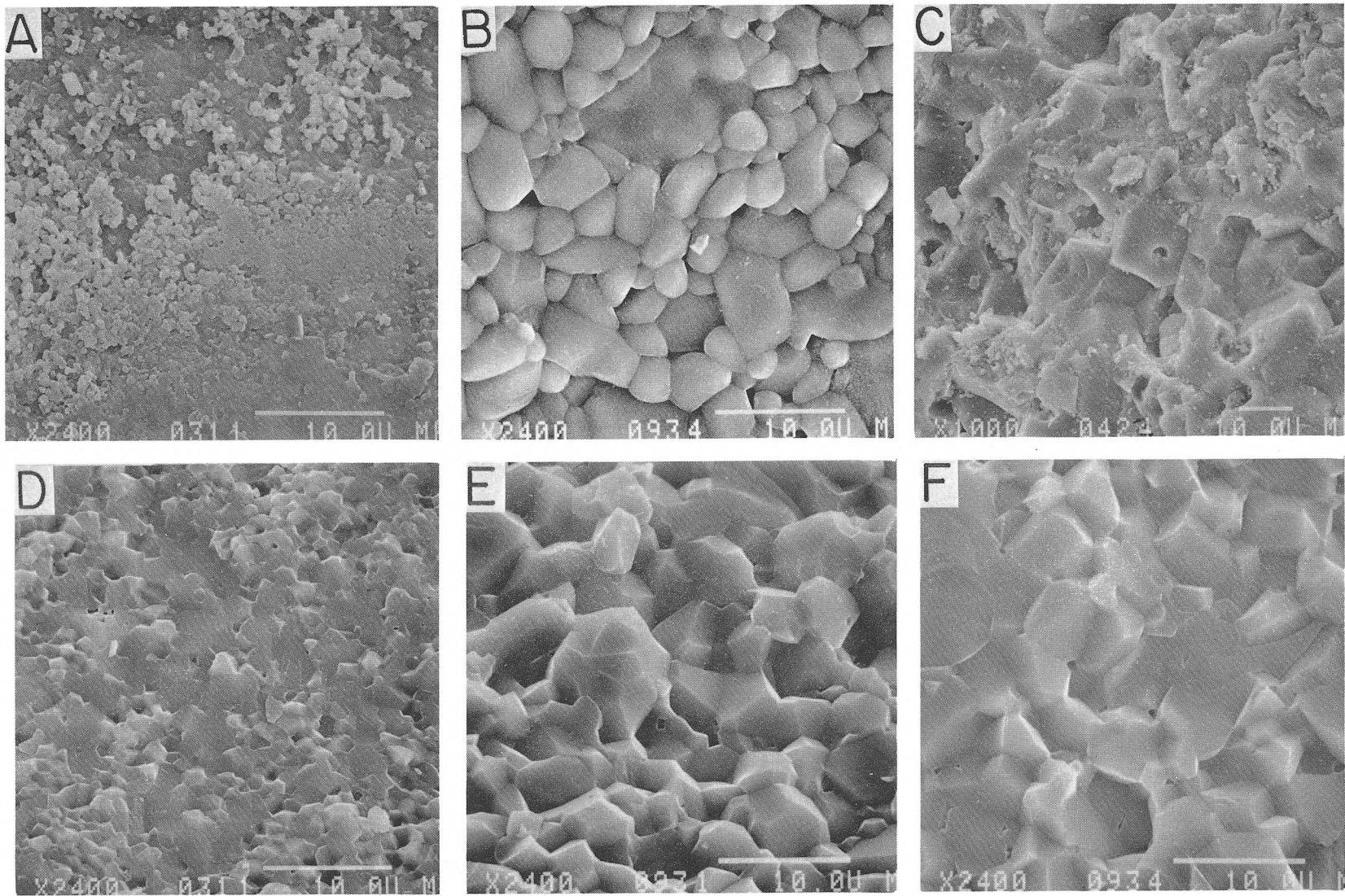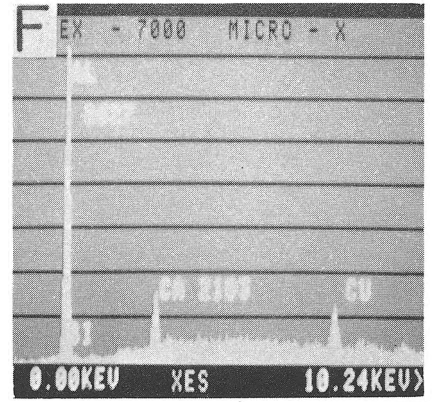
Fig. 8

Fig. 9
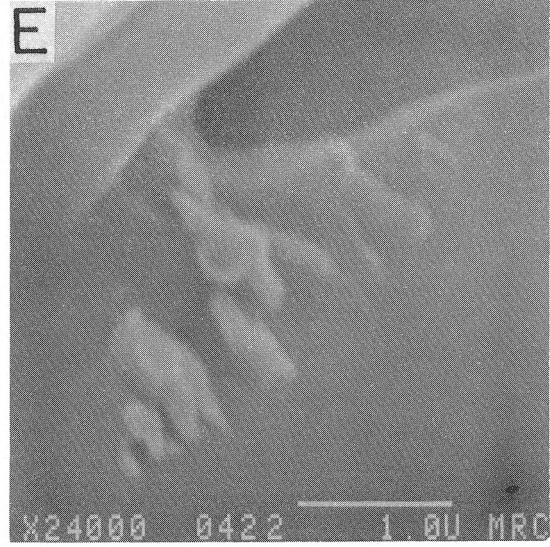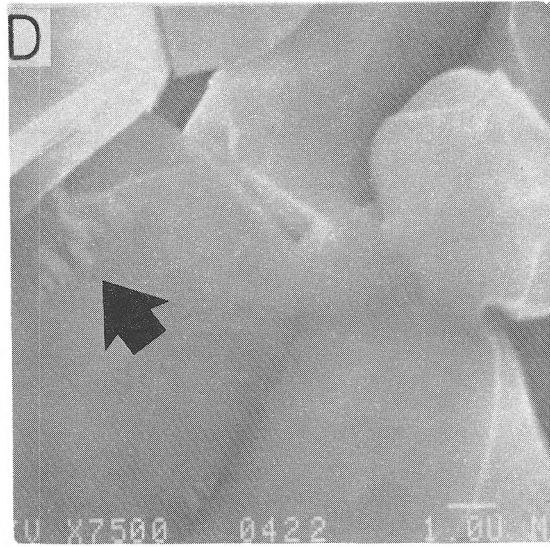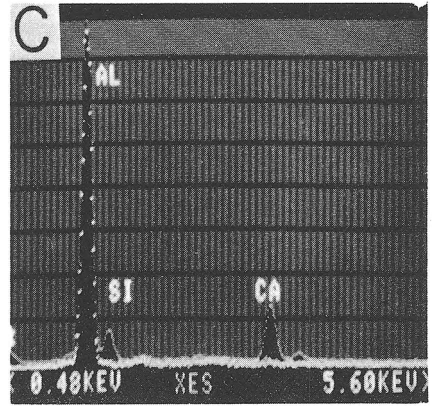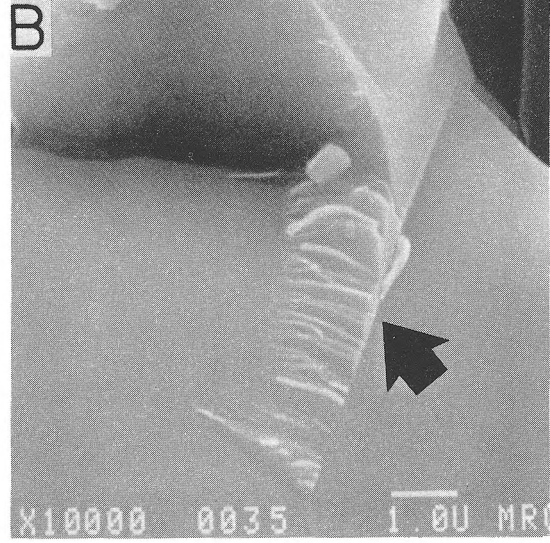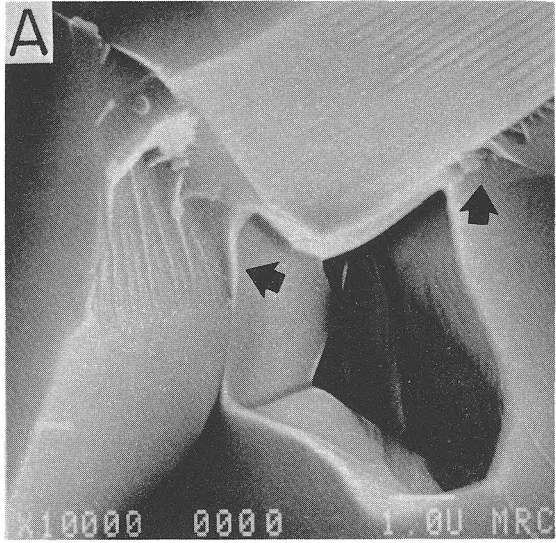
Fig. 10
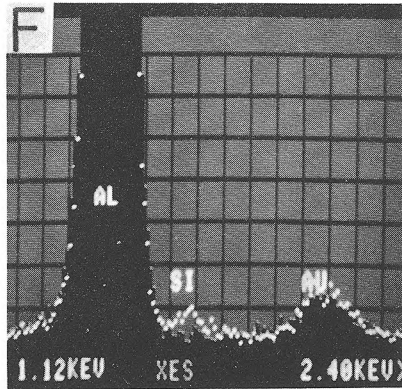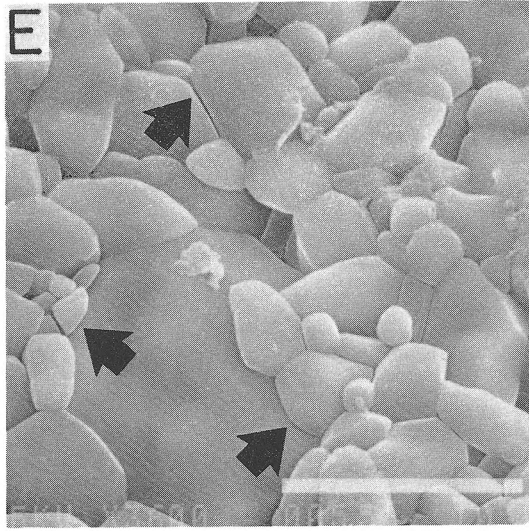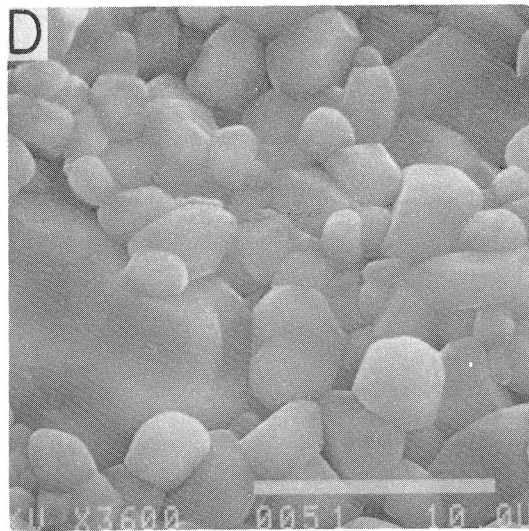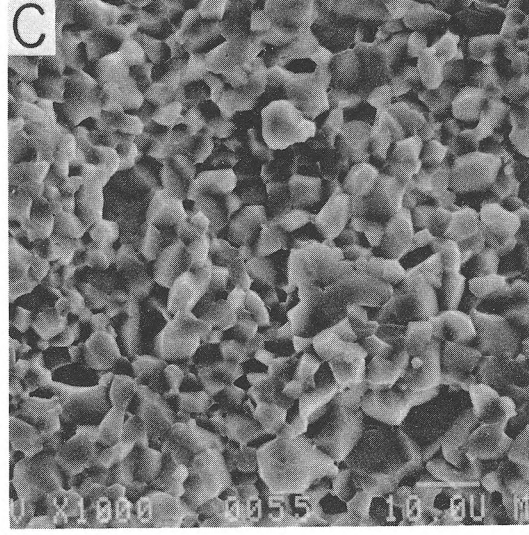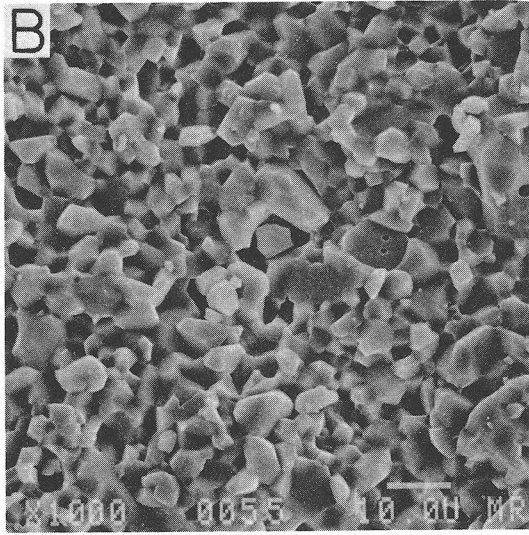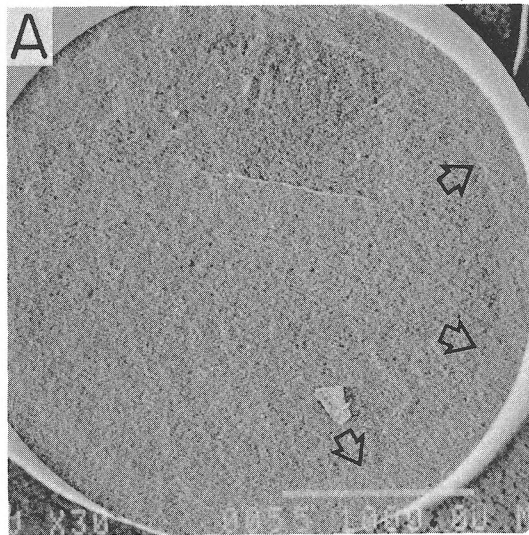
Fig. 11
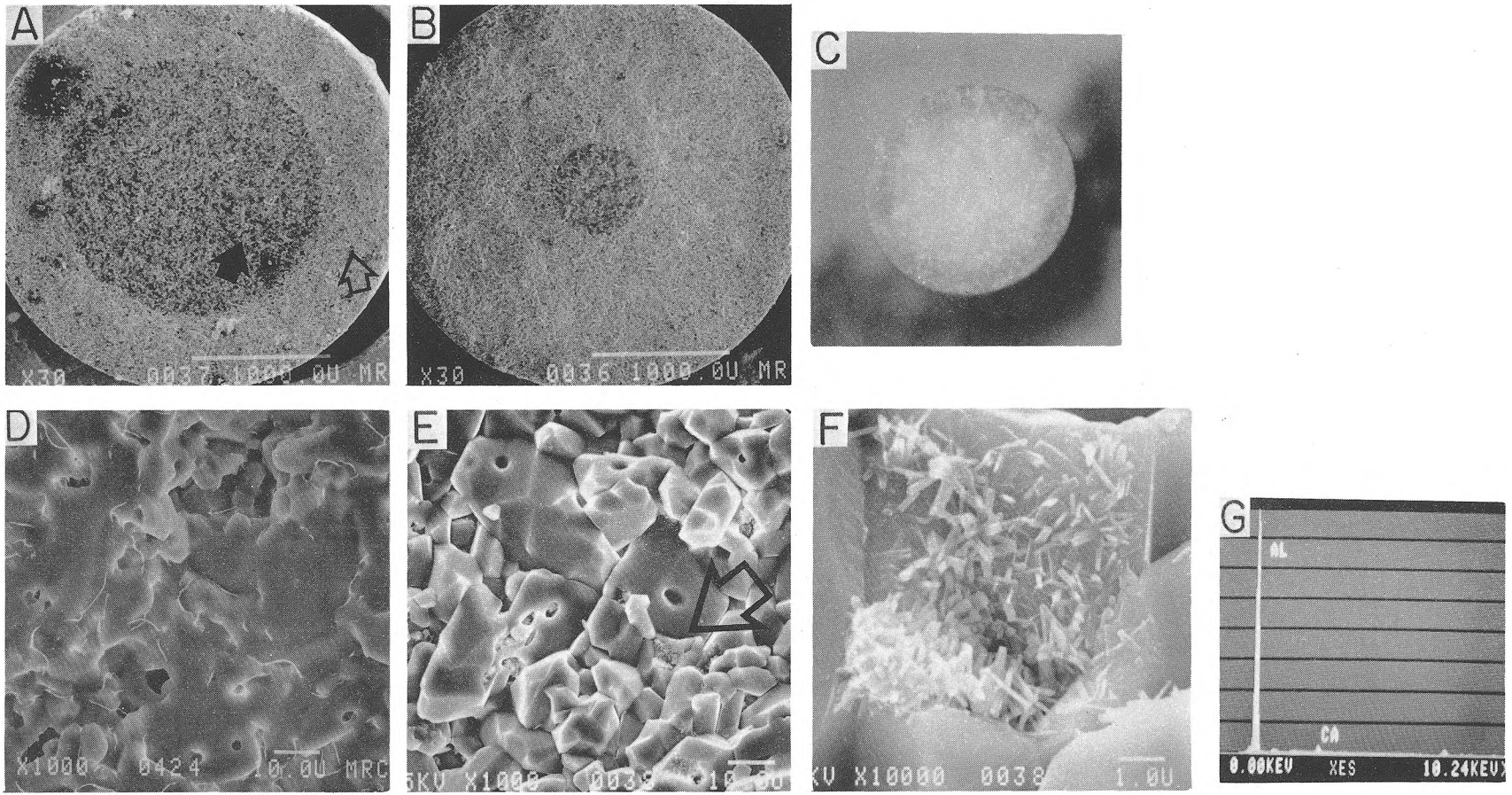
Fig. 12
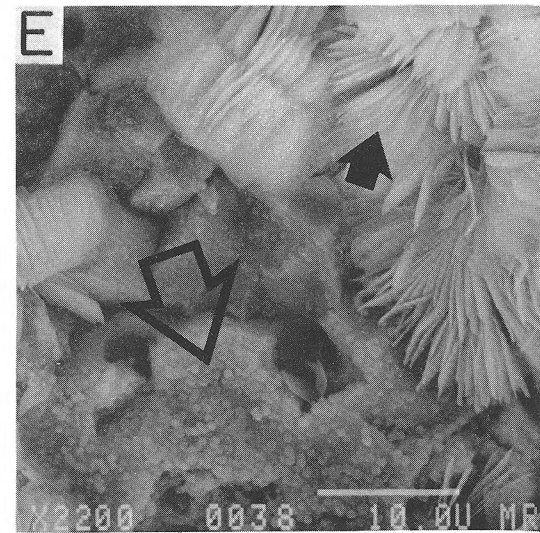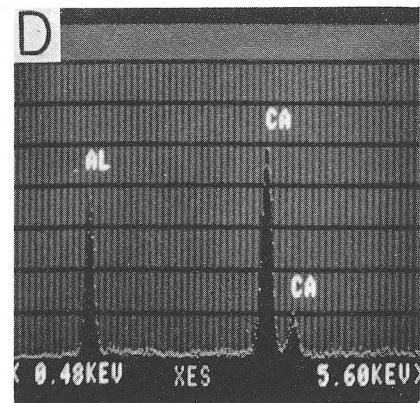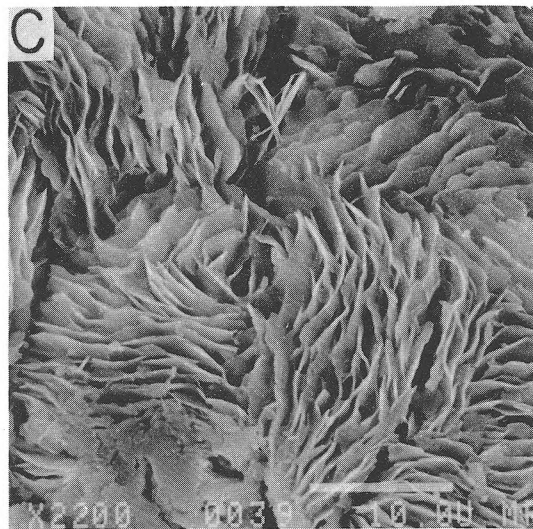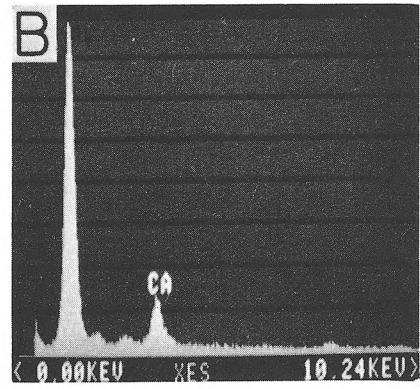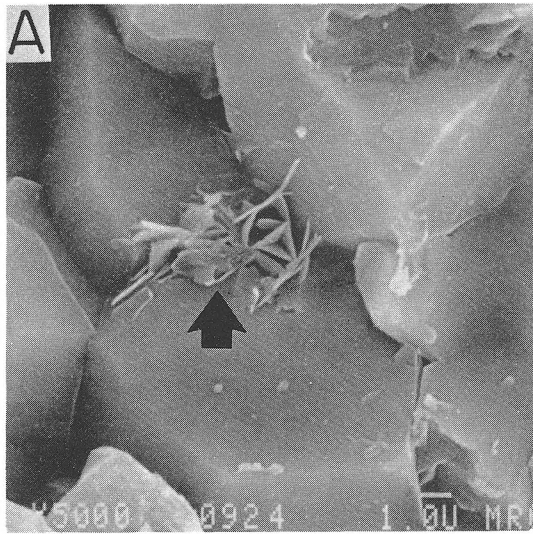
Fig. 13

VITA

Ho Tong Fang was born on December 12, 1956, in Taiwan, Republic of China. He received his primary education in Taiwan and in Singapore, and his secondary education in Ipoh, Malaysia and in Coleraine, Northern Ireland. He graduated from Imperial College, University of London, England with the degree of Bachelor of Science in Materials Science in July 1979.

He has been enrolled in the Graduate School of the University of Missouri-Rolla since August 1980 and has held a research assistantship.

APPENDIX A

Time to failure data for aluminas A, B, and C in demineralized water.

Alumina A

Tested at 37°C using 75% average fracture load (AFL).

N (total number of specimens) = 34.

Time (s)	Number of failure	Portion remained	$\ln\ln\frac{1}{1-F(t)}$ *
0	5	0.85	**
10	1	0.82	-3.49
35	1	0.79	-2.62
62	1	0.77	-2.25
120	1	0.74	-1.97
1.20×10^3	1	0.71	-1.68
1.80×10^3	1	0.68	-1.50
5.46×10^3	1	0.65	-1.34
5.32×10^5	1	0.62	-1.16
1.21×10^6 (2 wk)	21***	0.59	

  * $F(t) = i/1 + N$, where i is the rank of failure.

 ** Instant failures not included.

*** Number of specimens surviving the 2 wk testing period.

Alumina A

Tested at 70°C using 75% AFL.   N = 16.

Time (s)	No. of failure	Portion remained
0	5	0.69
120	1	0.63
1.80×10^3	1	0.56
1.84×10^4	1	0.50
8.30×10^4	1	0.44
1.85×10^5	1	0.38
3.13×10^5	1	0.31
6.43×10^5	1	0.25
1.21×10^6 (2 wk)	4***	0.19

*** Number of specimens surviving the 2 wk testing period.

Alumina B

Tested at 37°C using 75% AFL.

Time (s)	Number of failure	Portion remained	$\ln\ln\dfrac{1}{1-F(t)}$ *
0	3	0.77	**
2	1	0.69	-2.36
13	1	0.62	-1.62
210	1	0.54	-1.16
300	1	0.46	-0.81
3.03×10^3	1	0.39	-0.51
4.14×10^3	1	0.31	-0.23
5.37×10^3	1	0.23	0.02
4.09×10^4	1	0.15	0.24
4.79×10^4	1	0.08	0.54
9.80×10^5	1	0.0	0.88

 * F(t) = i/1 + N, where i is the rank of failure.
 ** Instant failures not included.

Alumina B

Tested at 70°C using 75% AFL.

Time (s)	No. of failure	Portion remained
0	9	0.57
18	1	0.52
42	1	0.48
210	1	0.43
300	1	0.38
390	1	0.33
480	1	0.29
1.20×10^3	1	0.24
1.38×10^3	1	0.19
1.98×10^3	1	0.14
6.60×10^3	1	0.10
1.68×10^4	1	0.05
2.59×10^4	1	0.0

Alumina C

Tested at 37°C using 75% AFL.   N = 24.

Time (s)	No. of Failure	Portion Remained	$\ln\ln\dfrac{1}{1-F(t)}$ *
0	1	0.74	**
5	1	0.71	-3.20
6	1	0.68	-2.36
7	1	0.64	-1.97
8	1	0.61	-1.68
10	1	0.58	-1.39
11	2	0.52	-1.22
15	1	0.48	-1.03
29	1	0.45	-0.84
35	1	0.42	-0.70
40	1	0.39	-0.58
59	1	0.36	-0.42
71	1	0.32	-0.31
90	1	0.29	-0.17
95	1	0.26	-0.06
120	1	0.23	0.05
150	1	0.19	0.19
210	1	0.16	0.30
240	1	0.13	0.41
270	1	0.10	0.57
360	1	0.07	0.71
720	1	0.03	0.88
2760	1	0.0	1.17

* $F(t) = i/1 + N$, where i is the rank of failure.
** Instant failures not included.

Alumina C

Tested at 70°C using 75% AFL.   N = 16.

Time (s)	No. of failure	Portion remained
0	14	0.13
1	1	0.07
30	1	0.0

Alumina C

Tested at 37°C using 65% AFL.   N = 12.

Time (s)	No. of failure	Portion remained
0	1	0.92
120	1	0.83
840	1	0.75
1.38×10^3	1	0.67
2.34×10^3	1	0.58
4.05×10^3	1	0.50
4.20×10^3	1	0.42
6.87×10^3	1	0.33
7.14×10^3	1	0.25
2.63×10^4	1	0.17
3.95×10^5	1	0.08
6.46×10^5	1	0.0

Alumina C

Tested at 37°C using 55% AFL. N = 13

Time (s)	No. of failure	Portion remained
2.46×10^3	1	0.92
1.21×10^6	12***	0.85

*** Number of specimens surviving the 2 wk testing period.

APPENDIX B

X-ray diffraction pattern of crystalline growth on the external surface of alumina C after aging 7 days at 37°C in 8 wt % HF.

| X-ray Pattern | | Identified Phases | |
d-spacing (Å)	Relative Intensity (1 to 5)	α-Al$_2$O$_3$ (corundum)	CaF$_2$ (Fluorite)
13.326	5		
11.071	2		
8.013	<1		
6.684	1		
5.754	3		
4.846	<1		
3.958	1		
3.675	1		
3.450	2	3.479 (75)*	
3.324	2		
3.145	4		3.153 (94)
3.045	4		
3.015	1		
2.886	2		
2.626	<1		
2.533	3	2.552 (90)	
2.368	2	2.379 (40)	
2.301	1		
2.225	2		

* Number in parenthesis denotes relative intensity (1-100).

Appendix B (Cont.)

2.073	3	2.085 (100)	
2.016	3		
1.966	5	1.964 (2)	1.931 (100)
1.925	1		
1.766	2		
1.738	2	1.740 (45)	
1.686	1		1.647 (35)
1.597	3	1.601 (80)	
1.578	<1		
1.529	<1		
1.508	1	1.510 (8)	
1.432	<1		
1.400	2	1.404 (30)	
1.370	2	1.374 (50)	1.366 (12)
1.300	<1		
1.236	1	1.239 (16)	
		1.234 (8)	

APPENDIX C

Ca concentration of demineralized water in contact with aluminas A and B for 21 days at 37° and 70°C.

	Blank Solution Demin. Water		Alumina A		Alumina B	
	37	70	37	70	37	70
Ca	0.003	0.011	0.037	0.069	0.215	0.249
Conc.	0.020	0.003	0.064	0.043	0.200	0.173
(ppm)	0.017	0.003	0.028	0.045	0.178	0.384
	0.003	0.023	0.046	nd	0.245	0.451
Mean	0.011 ±0.009*	0.010 ±0.009	0.044 ±0.015	0.052 ±0.014	0.209 ±0.028	0.314 ±0.130

nd = not detected

* ± values correspond to one standard deviation.

Specimen to water volume ratio ∿ 1:7